Current Research in Neurobiology 5 (2023) 100094

Contents lists available at ScienceDirect

Current Research in Neurobiology

journal homepage: www.sciencedirect.com/journal/current-research-in-neurobiology

Progranulin is an FMRP target that influences macroorchidism but not behaviour in a mouse model of Fragile X Syndrome

Benjamin Life [a,b], Luis E.B. Bettio [c], Ilse Gantois [d,e], Brian R. Christie [c,f,h], Blair R. Leavitt [a,b,g,h,*]

[a] Centre for Molecular Medicine and Therapeutics, Department of Medical Genetics, University of British Columbia, Vancouver, BC, V6H 0B3, Canada
[b] BC Children's Hospital Research Institute, Vancouver, BC, V5Z 4H4, Canada
[c] Division of Medical Sciences, University of Victoria, Victoria, BC, V8P 5C2, Canada
[d] Department of Biochemistry, McGill University, Montreal, H3A 2T5, Quebec, Canada
[e] Rosalind and Morris Goodman Cancer Research Centre, McGill University, Montreal, H3A 2T5, Quebec, Canada
[f] Island Medical Program, University of British Columbia, Victoria, BC, V8P 5C2, Canada
[g] Division of Neurology, Department of Medicine, University of British Columbia Hospital, Vancouver, BC, V6T 2B5, Canada
[h] Center for Brain Health, University of British Columbia, Vancouver, BC, V6T 1Z3, Canada

ARTICLE INFO

Keywords:
Progranulin
Fragile X Syndrome
Autism spectrum disorder
Neurodevelopment
Mouse models

ABSTRACT

A growing body of evidence has implicated progranulin in neurodevelopment and indicated that aberrant progranulin expression may be involved in neurodevelopmental disease. Specifically, increased progranulin expression in the prefrontal cortex has been suggested to be pathologically relevant in male *Fmr1* knockout (*Fmr1* KO) mice, a mouse model of Fragile X Syndrome (FXS). Further investigation into the role of progranulin in FXS is warranted to determine if therapies that reduce progranulin expression represent a viable strategy for treating patients with FXS. Several key knowledge gaps remain. The mechanism of increased progranulin expression in *Fmr1* KO mice is poorly understood and the extent of progranulin's involvement in FXS-like phenotypes in *Fmr1* KO mice has been incompletely explored. To this end, we have performed a thorough characterization of progranulin expression in *Fmr1* KO mice. We find that the phenomenon of increased progranulin expression is post-translational and tissue-specific. We also demonstrate for the first time an association between progranulin mRNA and FMRP, suggesting that progranulin mRNA is an FMRP target. Subsequently, we show that progranulin over-expression in *Fmr1* wild-type mice causes reduced repetitive behaviour engagement in females and mild hyperactivity in males but is largely insufficient to recapitulate FXS-associated behavioural, morphological, and electrophysiological abnormalities. Lastly, we determine that genetic reduction of progranulin expression on an *Fmr1* KO background reduces macroorchidism but does not alter other FXS-associated behaviours or biochemical phenotypes.

1. Background

Autism spectrum disorder (ASD; autism) is a heterogenous neurodevelopmental disorder characterized by restricted or repetitive behaviour and deficits in social ability (Lord et al., 2020). Autism is common, affecting 1 in 59 people in the United States and over 52 million people worldwide (Baxter et al., 2015; Baio et al., 2018). To begin untangling the diversity in clinical presentation of autism, efforts have been made to understand commonly occurring pathological mechanisms. In particular, the identification of genetic syndromes conferring significant risk for the development of autism, such as Fragile X Syndrome and Phelan-McDermid Syndrome (caused by mutations in the genes *FMR1* and *SHANK3*, respectively) have allowed for the development of animal models for autism (The Dutch-Belgian Fragile et al., 1994; Peça et al., 2011). While the identification of these and other autism-associated genes represents an important step forward in our understanding of autism pathology, much work remains to be done in understanding the downstream effects of mutations in these genes.

Fragile X Syndrome (FXS) is the leading monogenic cause of autism and intellectual disability, affecting 1 in 7000 males and 1 in 11,000 females worldwide (Hunter et al., 2014). FXS is the product of a CGG triplet repeat expansion in the 5′ untranslated region of the X-linked gene *FMR1* (Verkerk et al., 1991). This trinucleotide expansion causes

* Corresponding author. Centre for Molecular Medicine & Therapeutics, Department of Medical Genetics, University of British Columbia, B.C. Children's Hospital, 950 West 28th Avenue, Vancouver, BC, V5Z 4H4, Canada.
E-mail address: bleavitt@cmmt.ubc.ca (B.R. Leavitt).

https://doi.org/10.1016/j.crneur.2023.100094
Received 10 December 2022; Received in revised form 17 May 2023; Accepted 5 June 2023
Available online 16 June 2023

Abbreviations:

aCSF	Artificial cerebrospinal fluid
ASD	Autism Spectrum Disorder
BS	Brainstem
CA1	Cornu Ammonis 1
CER	Cerebellum
CNS	Central nervous system
CSF	Cerebrospinal fluid
DG	Dentate gyrus
FXS	Fragile X Syndrome
HIP	Hippocampus
LTP	Long term potentiation
MW	Molecular weight
MWM	Morris water maze
NF2	Normalization factor 2
NS	not significant
pFC	Prefrontal cortex
PND	Postnatal day
SEM	Standard error of the mean
Tg	Transgene
VPA	Valproic acid
WT	wild-type

promoter methylation and decreased *FMR1* expression (Pieretti et al., 1991; Verheij et al., 1993; Coffee et al., 1999, 2002). *FMR1* encodes Fragile X Messenger Ribonucleoprotein 1 (FMRP), an RNA-binding protein (Ashley et al., 1993; Siomi et al., 1993). FMRP is pleiotropic, regulating splicing, editing, and translation of target transcripts in addition to directly interacting with diverse classes of proteins such as ion channels, molecular motors, and other RNA-binding proteins (reviewed in Davis and Broadie, 2017). The absence of FMRP expression in humans and mice induces macroorchidism (Turner et al., 1975; Lachiewicz and Dawson, 1994), reduced cortical dendritic spine maturity, increased spine density (Rudelli et al., 1985; Hinton et al., 1991; Irwin et al., 2001), and abnormal synaptic plasticity in multiple brain regions (Huber et al., 2002; Zhao et al., 2005; Eadie et al., 2012; Bostrom et al., 2015; Li et al., 2002). These physiological changes are thought to stem from the dysregulated expression of FMRP's numerous target transcripts, including up to 4% of brain expressed genes (Ashley et al., 1993). A better understanding of the role of each target gene in the pathophysiology of FXS will help to inform rational therapeutic development.

The granulin precursor gene, progranulin (*GRN*), is widely expressed and implicated in many aspects of brain health maintenance. The role of progranulin in neurodegenerative disease is well established. Loss of a single copy of progranulin causes frontotemporal dementia (Baker et al., 2006; Cruts et al., 2006). Loss of both copies of progranulin causes a rare adolescent onset lysosomal storage disorder called neuronal ceroid lipofuscinosis (Smith et al., 2012; Kamate et al., 2019). Though a canonical function for progranulin remains elusive, progranulin appears capable of influencing neurite outgrowth (Van Damme et al., 2008; Laird et al., 2010), synaptic pruning (Lui et al., 2016), neuroinflammation (Martens et al., 2012; Yin et al., 2009), and lysosomal function (Elia et al., 2019; Paushter et al., 2018; Tanaka et al., 2017). Research into the impacts of aberrant progranulin expression during development will improve our understanding of progranulin's role in neurodevelopmental disease and shed light on progranulin's canonical functions.

Aberrant progranulin expression represents a potential pathophysiological mechanism in *Fmr1* KO mice, a mouse model of FXS. Increased progranulin mRNA and protein expression were observed in the medial prefrontal cortices but not hippocampi of *Fmr1* KO mice (Zhang et al., 2017). Furthermore, treatment of mouse neuronal cultures with recombinant mouse progranulin was sufficient to reproduce the FXS-associated phenotypes of increased dendritic spine density and reduced spine maturity observed in *Fmr1* KO neurons (Zhang et al., 2017). Acute reduction of progranulin expression following medial prefrontal cortex injection of lentivirus expressing short hairpin RNA targeted to progranulin reduced FXS-associated phenotypes in *Fmr1* KO mice. This targeted reduction of progranulin expression was reported to rescue FXS-associated long term potentiation (LTP) deficits, altered spine morphology, and behavioural phenotypes including open field hyperactivity and impaired trace fear conditioning (Zhang et al., 2017). Based on these promising results, we sought to expand the current understanding progranulin's role in FXS and autism.

In this work, we examine progranulin's involvement in FXS from several different angles. Progranulin upregulation in *Fmr1* KO mice is explored through the characterization of progranulin expression in 2-month-old *Fmr1* KO and wild-type mouse tissues. An FMRP RNA immunoprecipitation in two-week-old wild-type mice is performed to assess the extent of physical association between FMRP and progranulin mRNA. The hypothesis that increased progranulin expression alone is sufficient to cause FXS-associated phenotypes is evaluated through the characterization of progranulin over-expressing mice, referred to as GRN^{Tg} mice hereafter. These GRN^{Tg} mice express two copies of mouse progranulin and one copy of transgenic human progranulin of bacterial artificial chromosome origin inserted at the X-linked *Hprt* locus (Petkau et al., 2021). We previously demonstrated that human progranulin is appropriately expressed in GRN^{Tg} mice and functionally indistinguishable from mouse progranulin (Petkau et al., 2021). Finally, we assess the therapeutic benefit of a genetic reduction of progranulin expression on FXS-associated phenotypes in *Fmr1* KO mice. In concert, this work provides new insights into the role of progranulin in FXS and lays a foundation for further research into the effects of progranulin dysregulation in autism.

2. Methods

2.1. Breeding, genotyping, and husbandry of mice

All mice used in this study were on a C57BL/6J background. GRN^{Tg} mice were created as described previously (Petkau et al., 2021). *Fmr1* KO mice were purchased from Jackson Labs (Strain #003025) (The Dutch-Belgian Fragile et al., 1994). Separate colonies of GRN^{Tg} and *Fmr1* KO mice were maintained in house. In this manuscript, we use the term *Fmr1* KO to refer to male $Fmr1^{-/y}$ and female $Fmr1^{-/-}$ mice. Mice expressing wild-type *Fmr1* (male $Fmr1^{+/y}$ and female $Fmr1^{+/+}$ mice) are described hereafter as *Fmr1*+. Heterozygous females are referred to as $Fmr1^{+/-}$. The designation "wild-type" (or WT) is reserved for mice that express wild-type *Fmr1* and *Grn*, and do not contain the human progranulin transgene. For experiments assessing the effect of genetic reduction of progranulin expression on an *Fmr1* KO background, female $Fmr1^{+/-}$; $Grn^{+/+}$ mice were mated with male *Fmr1*+; $Grn^{+/-}$ mice to produce male littermates of the following genotypes: 1) *Fmr1*+; $Grn^{+/+}$, 2) *Fmr1*+; $Grn^{+/-}$, 3) *Fmr1* KO; $Grn^{+/+}$, and 4) *Fmr1* KO; $Grn^{+/-}$. The progranulin null allele in the $Grn^{+/-}$ mice has been described previously (Petkau et al., 2012). Mice were genotyped at wean and collection from tail DNA to determine the gene dosage of *Fmr1, Grn,* and GRN^{Tg} (see Supplementary Table 1 for primer sequences).

All mice were group housed with littermates to a maximum of five mice per cage in a pathogen-free barrier facility with a 12-h light/dark cycle. Cages contained shredded paper and plastic huts for enrichment, with food and water *ad libitum*. Behavioural tests were conducted in young adult animals, 2–3 months of age for the *Fmr1* KO; $Grn^{+/-}$

experiment and 2–6 months of age for the GRN^{Tg} vs wild-type experiment.

All animal work was approved by Animal Care Committees at the University of British Columbia and the University of Victoria in accordance with Canadian Council on Animal Care guidelines.

2.2. Quantitative RT-PCR for assessment of progranulin mRNA levels

Tissue samples were collected from male mice aged 2–3 months, snap frozen, and stored at −80 °C. Samples were thawed, placed in lysis buffer, and processed by bead homogenization. RNA was extracted from the tissue lysate following manufacturer's instructions (PureLink RNA mini kit; Invitrogen). RNA quantification was performed with a Nanodrop 1000 UV/VIS Spectrophotometer (Thermo Scientific). cDNA was generated from the reverse transcription of 500 ng of RNA per sample using the Superscript VILO kit (Invitrogen). The diluted cDNA (2.5 ng final input) was mixed with FastSYBR Green Master Mix (Applied Biosystems) and primers for *Grn*, *Csnk2a2*, *Gapdh, Paklip1,* or *Zfp91* (Supplementary Table 2) and measured in duplicate with a Step-One ABI System (Applied Biosystems). The mRNA expression of each gene was calculated using the standard curve method. For each tissue, the following control genes were analyzed: *Csnk2a2*, *Gapdh, Paklip1,* and *Zfp91*. Relative *Grn* expression was determined by dividing the quantity of *Grn* mRNA obtained from standard curve analysis to a normalization factor calculated for each sample by applying GeNorm (Vandesompele et al., 2002) to the quantity of control mRNA (*Csnk2a2*, *Gapdh, Paklip1,* or *Zfp91*) measured in each sample. Expression is reported as Relative Expression (NF2) to describe the use of the Normalization Factor (NF) calculated from the two most consistent control genes in each sample. The control genes used for each tissue are as follows: prefrontal cortex = *Csnk2a2* and *Zfp91,* brainstem = *Csnk2a2* and *Gapdh*, hippocampus = *Csnk2a2* and *Paklip1*, and lung = *Csnk2a2* and *Zfp91*.

2.3. Progranulin ELISA for assessment of protein expression

Tissue samples were obtained from 2–3-month-old male mice, snap frozen, and stored at −80 °C. Samples were homogenized in a lysis buffer of the following composition: 50 mM Tris-HCl, 1% Triton-X, 150 mM NaCl, 1% Halt Phosphatase Inhibitor Cocktail (Thermo Fisher Scientific), and 1% Halt Protease Inhibitor Cocktail (Thermo Fisher Scientific). Homogenized samples were centrifuged at 18,500×*g* for 5 min at 4 °C. The supernatants were decanted, aliquoted, and frozen at −80 °C. Total protein quantification for each sample was achieved by Bradford Assay using Quick Start™ Bradford 1x Dye Reagent (BioRad) and measured by a POLARstar Omega plate reader (BMG Labtech).

Mouse progranulin protein levels were quantified using an ELISA kit (mouse progranulin ELISA: cat. # ab219524, Abcam). For brain tissues, 50 μg of total protein was loaded per well; for peripheral tissues, 10 μg of protein was loaded. For cerebrospinal fluid, samples were limiting (2–5 μL were obtained from each mouse) so the maximum volume was added. Progranulin concentration in the cerebrospinal fluid was normalized per μL added. Progranulin expression in plasma was assayed in 100 μL of 1:250 diluted plasma. All tissue samples were evaluated in duplicate and normalized to reflect progranulin expression per 100 μg of total protein.

2.4. RNA immunoprecipitation

2.4.1. Tissue lysis

Cortical tissue was obtained from wild-type male mice aged to postnatal day 13, snap frozen, and stored at −80 °C. The tissues were then thawed on ice and homogenized using a Dounce homogenizer in 550 μL of ice-cold phosphate buffered saline. Cells were collected by centrifugation at 8600×*g* for 5 min at 4 °C. The supernatant was discarded, and the pellet was resuspended in 400 μL of complete polysome lysis buffer (100 mM KCl, 5 mM $MgCl_2$, 10 mM HEPES-NaOH pH 7, 0.5% Nonidet P-40 (NP-40), 1 mM dithiothreitol (DTT), 200 units/ml RNase OUT (10777019, Invitrogen), and 1% Halt Protease Inhibitor Cocktail). Cortical lysate was incubated on ice for 5 min prior to storage overnight at −80 °C.

2.4.2. Bead preparation

Immunoprecipitations were bead-based and adapted from the Pierce Crosslink Magnetic IP/Co-IP Kit (Cat. 88805, Thermo Scientific). Beads were prepared by conjugation with either rabbit anti-FMRP (ab17722, Abcam), or rabbit IgG control (12-370MI, MilliporeSigma). Bead preparation is as follows.

For each immunoprecipitation reaction, 1.8 mL of 1x Modified Coupling buffer was prepared by diluting 90 μL of 20x Coupling Buffer (Pierce Crosslink Magnetic IP/Co-IP Kit) and 90 μL of IP Lysis/Wash Buffer (0.025 M Tris, 0.15 M NaCl, 0.001 M EDTA, 1% NP-40, 5% glycerol, pH 7.4) with 1.62 mL of ultrapure water. The bottle of Pierce Protein A/G Magnetic Beads was briefly vortexed to obtain a homogeneous suspension from which 25 μL of bead solution was removed to a microcentrifuge tube. The tube was then placed on a magnetic stand to collect beads for 1 min. The storage solution was removed and discarded before rinsing the beads twice with 500 μL of 1x Modified Coupling Buffer. Concurrently, the FMRP and rabbit IgG control antibodies were diluted to a final concentration of 0.1 μg/μL with ultrapure water, 20x Coupling Buffer (diluted 1:20 to 1x final concentration), and IP Lysis/Wash Buffer (diluted 1:20). 100 μL of each of the prepared antibody solutions were then added to separate bead mixtures, gently mixed, and incubated on a rotating platform for 15 min at room temperature. To ensure that the beads stayed in suspension, the tubes were inverted every 5 min during incubation. The beads were then once again collected with a magnetic stand. The supernatant was removed and discarded. The beads were washed once in 100 μL 1x Modified Coupling Buffer and twice in 300 μL of 1x Modified Coupling Buffer. The antibody-coated beads were then resuspended in 900uL IP Lysis/Wash Buffer and incubated at 4 °C on a rotating tube holder until initiation of immunoprecipitations.

2.4.3. Immunoprecipitation

Cortical lysate was obtained from the −80 °C freezer, thawed and pelleted by centrifugation for 10 min at 18,500×*g*, 4 °C. Lysis supernatant was removed to a new microcentrifuge tube, pellets were discarded. Two 10 μL aliquots were removed from the lysate at this point, one was used in a Bradford assay to evaluate total protein concentration (as in the ELISA section) and the other was stored at −80 °C as an "Input" sample for use as a control in the downstream quantitative RT-PCR. Of the remaining cortical lysate, 100 μL was added to both the FMRP antibody-coated beads and the rabbit IgG-coated beads prepared above. The lysate/bead solutions were then incubated on a rotating wheel overnight at 4 °C.

Following the overnight incubation, the tubes were spun down briefly and placed on a magnetic rack in ice for 1 min. The supernatant was discarded. Tubes were then removed from the magnetic rack and 500 μL of ice-cold IP Lysis/Wash Buffer was added before the samples were vortexed vigorously. The tubes were returned to the ice-cold magnetic rack and incubated for 1 min after which the supernatant was discarded. This wash process was repeated five more times with 500 μL of ice-cold IP Lysis/Wash Buffer. Beads were then resuspended in 150 μL of "IP Lysis/Proteinase K Buffer" (IP Lysis/Wash buffer, 1% sodium dodecyl sulfate (SDS), and 1.2 mg/mL Proteinase K). Tubes were incubated at 55 °C for 30 min with gentle shaking to digest the proteins.

2.4.4. RNA extraction and cDNA synthesis

Following the above 30-min incubation, tubes were placed in the magnetic rack. At this time, supernatants were transferred to new tubes, to which 150 μL of IP Lysis/Wash Buffer was added. Beads were discarded. 300 μL of phenol: chloroform: isoamyl alcohol (125:24:1) was then added to each supernatant-containing tube. Samples were vortexed vigorously for 5 s then subjected to centrifugation at 18,500×*g* for 5 min

at room temperature to promote phase separation. 225 μL of the aqueous phase was carefully removed to a new tube without disturbing the protein interface. This process was then repeated once with the addition of 225 μL of phenol: chloroform: isoamyl alcohol (125:24:1) to the above supernatant-containing tubes and a second time with 450 μL chloroform. The organic phase was then discarded. To the tubes containing aqueous phase, the following solutions were added: 83.3 μL sodium acetate (3 M), 1.2 μL glycogen (20 mg/ml), and 820 μL of absolute ethanol. Samples were stored at −80 °C overnight to facilitate RNA precipitation.

The following day, samples were retrieved from the −80 °C freezer and centrifuged at 18,500×*g* for 30 min (4 °C). The supernatants were carefully removed and discarded without disturbing the pellets. The pellets were washed with 500 μL of cold 80% ethanol. Samples were vortexed to solubilize pellets, then subjected to centrifugation at 13,400×*g* for 15 min at 4 °C. Once again, the supernatants were carefully removed and discarded. Pellets were air-dried for 5 min at room temperature before resuspension in 20 μL of RNase-free water. RNA quantity was then assessed with a Nanodrop 1000 UV/VIS Spectrophotometer (Thermo Scientific). cDNA was generated from 14 μL of each immunoprecipitated RNA sample and 10 μL of each "Input" sample using the Superscript VILO kit (Invitrogen).

2.4.5. Quantitative RT-PCR

Quantitative RT-PCR was performed on the following samples: Input (diluted 1:10), FMRP RIP (diluted 1:10), Rb IgG (diluted 1:10), and a no template control. Primers specific to the following genes were used: *Map1b* (an established FMRP target) (Lu et al., 2004; Menon et al., 2008), *Gapdh* (an established non-target) (Zhang et al., 2007), and *Grn* (interaction with FMRP unknown) (Supplementary Table 2). FastSYBR Green Master Mix (Applied Biosystems) reagents were used, and samples were measured in duplicate with a Step-One ABI System (Applied Biosystems). C_T values were obtained and averaged between replicates. The C_T values for the Input samples were normalized by subtracting $\log_2(10)$ to account for the fact that the Input samples received 10% of the amount of lysate used in the immunoprecipitations. Fold enrichment of *Grn* was calculated relative to *Gapdh* for each sample of cortical lysate with the following formula:

$$\text{Fold enrichment of } Grn \text{ relative to } Gapdh = \frac{2^{\left(C_{T\,Input(Grn)} - C_{T\,RIP(Grn)}\right)}}{2^{\left(C_{T\,Input(Gapdh)} - C_{T\,RIP(Gapdh)}\right)}}$$

Fold enrichment of *Map1b* was calculated relative to *Gapdh* with the same formula, replacing the *Grn* values with those obtained from the *Map1b* reactions. Fold enrichment data is presented as n = 5, with each data point representing cortical lysate obtained from a unique mouse. Data is presented from three independent experiments.

2.5. Behavioural tests

Body weight was evaluated at 2 months of age. Hyperactivity in open field was assessed in 50 cm × 50 cm boxes with a test duration of 10 min and quantified by video analysis using EthoVision XT 14 (Noldus) (LPJJSpink et al., 2001), as previously described (Petkau et al., 2021). Open field testing in the *Fmr1* KO; $Grn^{+/-}$ experiment was conducted in a lit room. Elevated plus maze, a measure of anxiety-like behaviour, was assessed with a testing duration of 5 min and quantified with EthoVision XT 14 (Noldus). (LPJJSpink et al., 2001). Data is reported as the percentage of time in open arms divided by time in enclosed arms. Repetitive behaviour engagement was assessed by marble burying as follows. Mice were placed in a clean cage with 2 inches of familiar bedding upon which 15 evenly spaced marbles were placed. After a test duration of 30 min, mice were removed to their home cage and marbles that were 2/3 covered by bedding (manual inspection) were counted as buried. The Morris water maze test (used to assess spatial learning and memory) was conducted as described previously (Petkau et al., 2012, 2021). Sociability was assessed by the three-chamber test. Experimental mice were given 5 min of habituation time in the three-chamber apparatus. Two cylindrical wire cups are present in the apparatus, one in each non-centre room, and are empty during the habituation phase. The experimental mouse is then corralled into the centre room and a mouse and object (a di 2 inches × 2 inches x 2 inches) were added to the left and right wire cups, respectively. The experimental mouse is then given 5 min to explore before being corralled again. At this time, the di is replaced with a novel mouse and a third and final 5-min trial takes place. Interaction time is defined as time in which the experimental mouse is within one body length of a wire cage and is scored manually from video. Interaction partner mice were male wild type animals from an independent litter.

Inclusion and exclusion criteria for behavioural studies were established *a priori*. Inclusion criteria for these tests included that the mice be young adult (aged 2–6 months) and of the appropriate genotype for the experiment. Mice were excluded from these tests if they were visibly sick or had lost more than 20% of their body weight. Further exclusion criteria existed for the elevated plus maze, the Morris water maze, and the three-chamber test. If mice fell off the elevated platform, they were excluded from elevated plus maze testing. Five mice were excluded from the elevated plus maze test in the *Fmr1* KO; $Grn^{+/-}$ experiment due to falling from the platform, including two wild type animals and three *Fmr1* KO; $Grn^{+/+}$ animals. Mice that exclusively exhibited thigmotaxis during the Morris water maze training were excluded from testing. Mice that failed to enter all three chambers during the habituation phase of the three-chamber test were excluded. No mice were excluded from this study due to visible sickness, weight loss, thigmotaxis in Morris water maze, or failure to explore in the three-chamber test.

Randomization of testing order and cage location was not included in this study. The researcher conducting the behavioural tests (BL) was blinded to the genotypes of the animals. Analysis of behaviour data was performed by BL upon completion of the study and subsequent unblinding.

2.6. Golgi-cox analysis

Following decapitation, brains were removed from postnatal day 13 wild-type and GRN^{Tg} male mice. The brains were immersed in Golgi–Cox fixative solution (1% KCr_2O_7, 1% $HgCl_2$ 0.75% K_2CrO_4) and stored for 12 days at room temperature with a single solution change at 47 h. After day 12, the brains were rinsed in distilled water for 5 min then immersed in 70% ethanol for 24 h, 96% ethanol for 17 h, 100% ethanol for 7 h, and finally 1:1 ethanol: diethyl ether for 17 h. Brains were then embedded in parlodion (VWR, 100504-176) through incubation in gradually increasing concentrations of parlodion (3% parlodion for 9 days, 6% parlodion for 2 days, and 12% parlodion overnight). Embedded brains were cut into 100 μm sections using a vibratome. Sections encompassing the brain regions of interest (dorsal CA1 of the hippocampus and the somatosensory cortex) were selected for staining. The staining process is as follows: 5 min rinse in ddH2O, 30 min in 16% ammonia, 2 min rinse in ddH2O, 7 min in 1% sodium thiosulphate, 10 min rinse in ddH2O and dehydration in a graded series of ethanol (70% ethanol 1 min, 95% ethanol 1 min, and 100% ethanol 1 min). Sections were then exposed to 1:1 ethanol: diethyl ether to dissolve the parlodion, rinsed in 100% ethanol, then immersed in xylenes for 30 s before being mounted on slides and cover slipped with Cytoseal (Electron Microscopy Sciences, PA). For sections containing the dorsal CA1, this region was traced and pyramidal neurons that were clearly stained were identified. For sections containing the somatosensory cortex, this region was traced and stained pyramidal neurons in layer V were selected.

Ten neurons were traced from every mouse (n = 7 wild-type mice, n = 5 GRN^{Tg} mice) from no fewer than 3 different sections per mouse. Neurons were traced using a camera lucida attached to the microscope at a magnification of 100× (DMLS, Zeiss Microscope). The density of dendritic spines was estimated by annotating all visible spines on the

segments of basal dendrites with an appropriate branch order (orders 1–6) and a length ≥10 μm at 100x magnification. All visible spines were traced and morphologically characterized manually using Neurolucida 9.0 software (MBF Bioscience, VT). No attempt was made to correct for spines hidden beneath or above the dendritic segment, so the spine density values are likely to underestimate the actual density of the dendritic spines. Branch length, spine density, and spine morphology are reported as mean ± SEM from each mouse and summarize measurements from n = 70 wild-type neurons and n = 50 GRN^{Tg} neurons.

2.7. Electrophysiological recordings

2.7.1. Slice preparation

Adult male mice (55–65 days old) were anaesthetized with isoflurane, their brains removed, and transverse hippocampal slices were prepared as previously described (Vasuta et al., 2007; Yau et al., 2019). Briefly, transverse hippocampal slices (350 μm) were acquired using a Vibratome 1500 (Ted Pella, Inc., Redding, CA, United States). For sectioning, the brain was immersed in oxygenated (95% O_2/5% CO_2) artificial cerebrospinal fluid (aCSF) containing (in mM) 125 NaCl, 3 KCl, 1.25 $NaHPO_4$, 25 $NaHCO_3$, 1 $CaCl_2$, 6 $MgCl_2$, and 25 glucose at 4 °C. After sectioning, individual slices were transferred to a holding chamber, constructed from 12-hole well plates to allow slices to be kept in order. The holding chambers contained warm (32 °C) oxygenated aCSF consisting of (in mM) 125 NaCl, 2.5 KCl, 1.25 $NaHPO_4$, 25 $NaHCO_3$, 2 $CaCl_2$, 1.3 $MgCl_2$, and 10 dextrose. Slices were incubated at 32 °C for 30 min before being held at room temperature until used.

2.7.2. Field electrophysiology

Individual slices were transferred to a recording chamber and perfused with aCSF (32 °C; 2 ml/min). Electrodes were then visually positioned with the aid of an upright Olympus BC51WI microscope and motorized micromanipulators (Siskyou Design, USA). A concentric bipolar stimulating electrode (FHC, Bowdoin, ME) was used to activate fiber pathways with a short current pulse (120 μs; 10–40 μA) using a stimulus isolation unit (Getting Instruments). Field EPSPs were recorded using a borosilicate glass microelectrode (1 MΩ; filled with aCSF) and using a Multiclamp 700B amplifier (Molecular Devices, USA). Recordings from the dentate gyrus (DG) were conducted with both electrodes visually positioned about 200–250 μm from the cell layer in the medial perforant path. For DG recordings only, the $GABA_A$ receptor antagonist bicuculline methiodide was added to the aCSF prior to the application of conditioning stimuli (5 μM; Sigma-Aldrich, ON, Canada) to help reduce feedback inhibition. Recordings from the CA1 region were conducted with both electrodes positioned about 300 μm from the pyramidal cell layer in the Schaffer collateral pathway. Electrode spacing was approximately 200–300 μm in both regions, and experiments were performed with the EPSP amplitude set at 50% of the maximum response. Stable recordings were required for a period of at least 15 min prior to the application of conditioning stimuli. LTP was induced by applying a high frequency conditioning stimulus (4 trains of 50 pulses at 100 Hz, at 30 s intervals). Post-conditioning responses were then recorded for 60 min.

2.8. Western blot analysis

Cortical tissue samples were collected from $n = 8$ *Fmr1*+; $Grn^{+/+}$, *Fmr1* KO; $Grn^{+/+}$, and *Fmr1* KO; $Grn^{+/-}$ mice at three months of age. Samples were homogenized and processed as in the ELISA section, though a different lysis buffer was utilized: 50 mM Tris-HCl, 1% Triton-X, 150 mM NaCl, 0.1% Sodium Dodecyl Sulfate, 1% Ethylenediaminetetraacetic acid, 1% Sodium deoxycholate, 1% Halt Phosphatase Inhibitor Cocktail (Thermo Fisher Scientific), and 1% Halt Protease Inhibitor Cocktail (Thermo Fisher Scientific). Western blots were performed for FMRP to assess FMRP expression and for MMP9, ERK, and pERK to probe for FXS-associated dysfunction in the MAPK/ERK pathway (Sidhu et al., 2014; Wen et al., 2018; Sawicka et al., 2016; Wang et al., 2012). For each sample, 30 μg of cortical lysate was denatured in LDS sample buffer (Invitrogen, Carlsbad, CA, United States) with 100 mM dithiothreitol and heated to 95 °C for 10 min. Samples were loaded on a 12% bis-tris gel and exposed to 150V for 45 min. Samples were then transferred to 0.45 mm nitrocellulose membranes overnight at 4 °C. Membranes were blocked with 5% milk in tris-buffered saline (TBS) for 2 h, washed three times for 10 min each in TBS + 0.05% Triton X (TBS-T), and stained overnight at 4 °C with one of the following target antibodies: rabbit anti-MMP9 (1:1000, #13667 Cell Signalling Technologies), rabbit anti-ERK (1:1000, #4695 Cell Signalling Technologies), rabbit anti-phospho-ERK (1:2000, #4370 Cell Signalling Technologies), or rabbit anti-FMRP (1:2000, ab17722, Abcam). Immunoblots were then washed three times in TBS-T and incubated for 2 h at room temperature with 1:4000 IRDye® 800CW Goat anti-Rabbit IgG Secondary Antibody (926–32211, Li-Cor). Immunoblots were then washed again prior to imaging with the Li-Cor Odyssey Infrared Imaging System. Subsequently, the immunoblots were stained for the loading control using 1:3000 mouse anti beta-tubulin (G098, abm) and 1:4000 IRDye® 680RD Goat anti-Mouse IgG Secondary Antibody (926–68070, Li-Cor) or 1:3000 rabbit anti-calnexin (C4731, Sigma-Aldrich) and 1:4000 IRDye® 680RD Goat anti-Rabbit IgG Secondary Antibody (926–68071, Li-Cor).

2.9. Statistical analyses

All statistical analyses were performed in GraphPad 9.1.2. For normally distributed data with similar variance and a single variable, comparisons of two groups were analyzed by unpaired *t*-test. Comparisons of three or more groups were analyzed by one-way ANOVA followed by Dunnett's post-hoc test with all means being compared to the wild type (control) mean. A two-way ANOVA followed by Šídák's multiple comparisons test was used when two or more groups were being evaluated for two variables (as in Morris water maze training, spine morphology, and the *Fmr1* KO; $Grn^{+/-}$ experiments). Supplementary Table 3 contains descriptive statistics for all figures. Supplementary Table 4 contains further statistics for the two-way ANOVAs in Fig. 5 and Fig. S11. This work uses a significance threshold of p-value less than 0.05.

3. Results

To better understand the role of progranulin in FXS, we characterized progranulin expression in *Fmr1* KO mice. Progranulin protein expression was assessed by ELISA in 2-month-old *Fmr1* KO and wild-type mice (Fig. 1). Progranulin protein was found to be upregulated in *Fmr1* KO mouse prefrontal cortex, brainstem, liver, and lung (Fig. 1A and B). Conversely, progranulin protein expression was not distinguishable from wild-type in *Fmr1* KO mouse cerebellum, hippocampus, spleen, heart, testes, cerebrospinal fluid, plasma, thalamus, and hypothalamus (Fig. 1, Fig. S1). To determine whether the increased progranulin expression in *Fmr1* KO mice is pre- or post-transcriptional, progranulin mRNA was assessed in a subset of tissues. Whilst progranulin protein expression was increased in the prefrontal cortex, brainstem, and lung, progranulin mRNA expression was not found to be increased in these tissues (Fig. S2). Nor was progranulin mRNA increased in the hippocampus (Fig. S2). Thus, the phenomenon of increased progranulin expression in *Fmr1* KO mice is tissue-specific and post-transcriptional.

Given that progranulin expression is increased post-transcriptionally in the absence of FMRP, we hypothesized that progranulin mRNA is a target of FMRP. FMRP is known to act as a translational repressor to target genes via direct interaction with target mRNA (Laggerbauer et al., 2001; Darnell et al., 2011; Li et al., 2001). Therefore, we probed for a physical interaction between FMRP and progranulin mRNA by RNA immunoprecipitation. Briefly, cortical lysate from five wild-type male mice at postnatal day 13 was subjected to immunoprecipitation using an

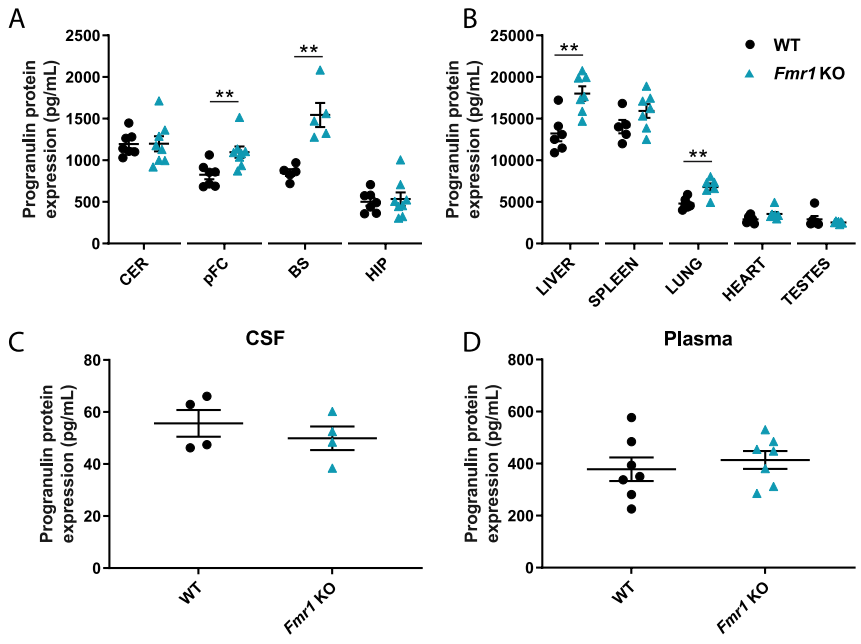

Fig. 1. Progranulin protein expression is increased in the *Fmr1* KO mouse prefrontal cortex, brainstem, liver, and lung. Mouse progranulin protein expression is measured by ELISA in multiple CNS and peripheral tissues of wild-type (black circles) and *Fmr1* KO (teal triangles) mice. A) Progranulin expression in the cerebellum (CER) (WT n = 7, *Fmr1* KO n = 8), prefrontal cortex (pFC) (WT n = 7, *Fmr1* KO n = 8), brainstem (BS) (WT n = 5, *Fmr1* KO n = 5), and hippocampus (HIP) (WT n = 7, *Fmr1* KO n = 8). B) Progranulin expression in the liver (WT n = 6, *Fmr1* KO n = 7), spleen (WT n = 5, *Fmr1* KO n = 7), lung (WT n = 6, *Fmr1* KO n = 6), heart (WT n = 6, *Fmr1* KO n = 7), and testes (WT n = 6, *Fmr1* KO n = 7). C) Progranulin expression in the cerebrospinal fluid (CSF) (WT n = 4, *Fmr1* KO n = 4). D) Progranulin expression in the plasma (WT n = 7, *Fmr1* KO n = 7). Concentrations are normalized to 100ug of protein added. Data are presented as mean ± standard error of the mean (SEM). **p < 0.01 by unpaired *t*-test.

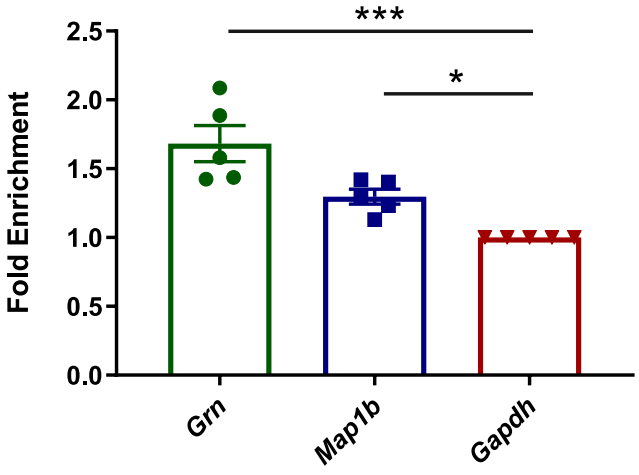

Fig. 2. Progranulin mRNA associates with FMRP by RNA immunoprecipitation. RNA immunoprecipitation was performed on cortical lysate from n = 5 post-natal day 13 male wild-type mice using an FMRP-specific antibody. mRNA levels of Progranulin (*Grn*), *Map1b*, and *Gapdh* are quantified by qPCR and reported as fold enrichment relative to *Gapdh*. Data are presented as mean ± standard error of the mean (SEM). *p < 0.05, ***p < 0.001 by one-way ANOVA with Dunnett's multiple comparisons test.

FMRP-specific antibody under native, non-crosslinking conditions. cDNA was then synthesized from the precipitated mRNA. Enrichment of progranulin mRNA was compared to enrichment of *Map1b* (an established FMRP target) (Lu et al., 2004; Menon et al., 2008) and *Gapdh* (an established non-target) (Zhang et al., 2007) (Fig. 2). Indeed, *Map1b* was found to be significantly enriched relative to *Gapdh*, demonstrating the functionality of this assay (Fig. 2). Strikingly, progranulin mRNA was found to be highly enriched relative to *Gapdh,* (Fig. 2)*,* indicating that FMRP interacts with progranulin mRNA.

Having further described the relationship between progranulin and FMRP and encouraged by previous reports of the pathological significance of progranulin over-expression in *Fmr1* KO mice (Zhang et al., 2017), we sought to determine if increased progranulin expression during development is sufficient to cause the autistic-like phenotypes observed in *Fmr1* KO mice. To this end, we endeavoured to characterize the early adulthood behaviour and brain physiology of GRN^{Tg} mice. These mice express progranulin at increased levels and FMRP at wild-type levels. Previous longitudinal characterization of the GRN^{Tg} mice has found them to be largely normal (Petkau et al., 2021). However, in-depth early adulthood assessments of behaviour, electrophysiology, and synaptic morphology have not previously been performed.

We first evaluated body weight and a panel of autism-associated behaviour tests in male and female GRN^{Tg} and wild-type mice. We report no difference in 2-month body weight between male GRN^{Tg} and wild-type mice (Fig. 3A). In the open field test, an assessment of hyperactivity, we observed an increase in activity in male GRN^{Tg} mice (n = 39) at two months of age (Fig. S3). This hyperactivity phenotype, while statistically significant, is subtle. Power calculations suggest that n = 41 is required to observe hyperactivity in male GRN^{Tg} mice at 80% power. Consistent with this subtlety, we report a trend toward increased hyperactivity that did not reach statistical significance (p = 0.08) in an independent cohort of male GRN^{Tg} mice (n = 18) (Fig. 3B). We include both sets of data for transparency. However, the remaining tests were conducted in the subsequent independent cohort, so they are all presented together in Fig. 3. GRN^{Tg} mice were not found to exhibit the anxiety deficits in elevated plus maze that have been reported in *Fmr1* KO mice (Fig. 3C), (Saré et al., 2016; Liu et al., 2011; Yuskaitis et al., 2010; Heulens et al., 2012; Hébert et al., 2014) though this is consistent with prior observations of no *Fmr1* KO genotypic differences in this test (Yan et al., 2004; Nielsen et al., 2002; Mineur et al., 2002; Kazdoba et al., 2014). No increased repetitive behaviour engagement was observed in male GRN^{Tg} mice, as assessed by the marble burying test (Fig. 3D). Spatial learning and memory in the Morris water maze was found to be normal in male GRN^{Tg} mice (Fig. 3E and F). Parallel characterization of female GRN^{Tg} and wild-type mice yielded a similar mildness of behavioural phenotypes. GRN^{Tg} female mice displayed reduced marble burying activity (Fig. S4D) in the absence of other behavioural changes (Fig. S4). No macroorchidism was observed in the GRN^{Tg} male mice (Fig. S5). Aside from the mild hyperactivity phenotype observed in male GRN^{Tg} mice and marble burying deficits in female GRN^{Tg} mice, we conclude that a genetic increase in progranulin expression during development is insufficient to cause FXS-associated autistic-like

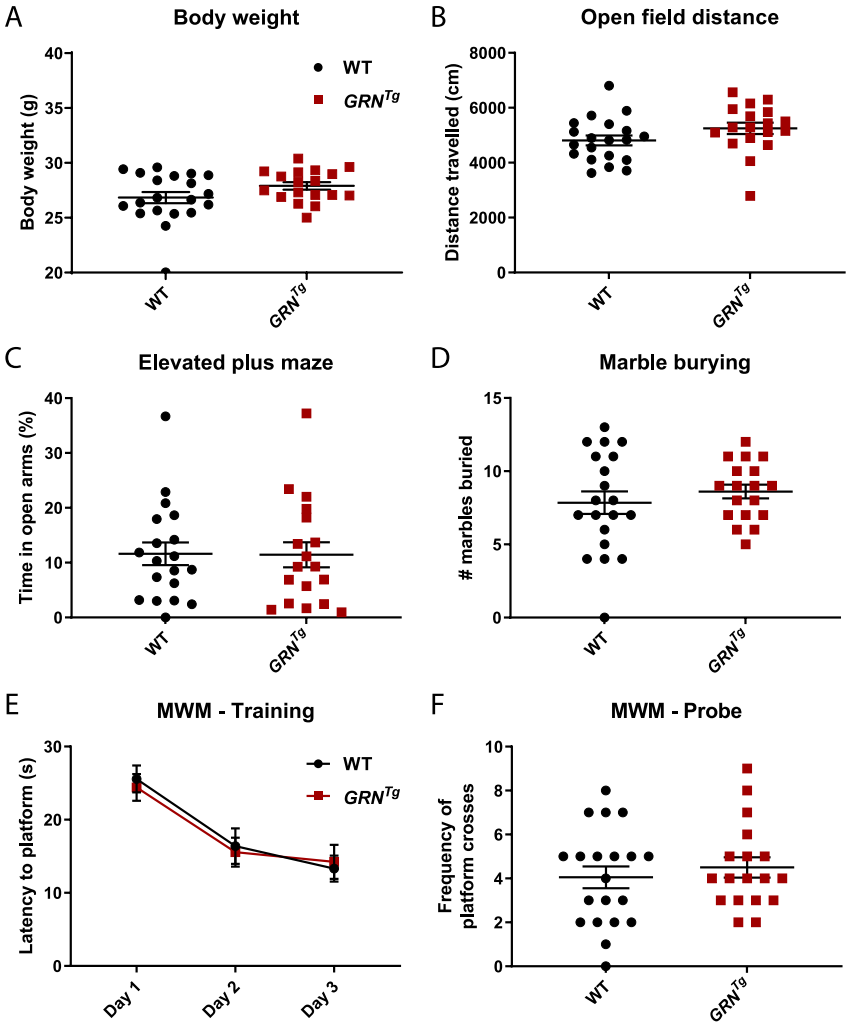

Fig. 3. Genetic over-expression of progranulin throughout development does not cause autistic-like behavioural phenotypes commonly reported in *Fmr1* KO mice. Male wild-type (black) and *GRN*^{Tg} mice (red) are characterized by body weight (A), open field test (B), elevated plus maze (C), marble burying (D), and Morris water maze (MWM) (E, F). Wild-type mice are characterized at n = 20 for all tests except elevated plus maze, where one mouse was excluded. *GRN*^{Tg} mice are characterized at n = 18 for all tests. Mice are age matched, with tests performed from 2 to 5 months of age. Data are presented as mean ± standard error of the mean (SEM). Data are analyzed by unpaired *t*-test for A-D, F and two-way ANOVA for E. No significant difference is observed in any comparison. (For interpretation of the references to colour in this figure legend, the reader is referred to the Web version of this article.)

behaviour, altered cognitive ability, or morphological changes reported in *Fmr1* KO mice.

We further examined synaptic morphology and electrophysiology in *GRN*^{Tg} mice to determine if increased progranulin during development modified brain physiology independent of profound behavioural changes. Synaptic morphology was assessed in postnatal day 13 male *GRN*^{Tg} and wild-type mice by Golgi-cox staining in two regions of interest in *Fmr1* KO mice, the CA1 (Fig. 4) and prefrontal cortex layer V (Fig. S6). (Nimchinsky et al., 2001; Su et al., 2011; Bilousova et al., 2009; He and Portera-Cailliau, 2013) Briefly, brains were collected, stained with Golgi-cox solution, and cut in 100 μm sections. Stained pyramidal neurons were identified in the CA1 and prefrontal cortex layer V. Dendritic branches and spine classifications were manually annotated for ten neurons per brain region per mouse (n = 5 GRN^{Tg} mice and n = 7 wild-type mice). No changes to spine density, branch length, or spine maturity were observed in either the CA1 (Fig. 4A–C) or layer V of the somatosensory cortex (Fig. S6). In support of these findings, LTP deficits were also not detected in 2-month-old *GRN*^{Tg} mice in either the CA1 (Fig. 4D), or the dentate gyrus (Fig. S7), subfields. While we cannot conclude that increased progranulin expression has no effect on neurodevelopment, it is clear that the increased expression in this model system is not sufficient to phenocopy several of the most commonly described neurophysiological deficits in *Fmr1* KO mice.

After showing that increased progranulin expression alone is insufficient to cause gross autistic-like phenotypes in mice, we sought to determine if increased progranulin expression is a necessary component of autism. To this end, we queried progranulin protein expression in another mouse model of autism, *Shank3B*– KO mice (Peça et al., 2011), referred to as *Shank3* KO mice hereafter. Deletion of the postsynaptic protein *Shank3* has been found to cause autism in humans (Durand et al., 2007; Moessner et al., 2007; Gauthier et al., 2009; Waga et al., 2011) and autistic-like phenotypes in mice (Peça et al., 2011; Wang et al., 2011). While increased progranulin protein expression was detected in the prefrontal cortex and brainstem of 2-month old *Fmr1* KO mice (Fig. 1), no increased expression was observed in these tissues in *Shank3* KO mice of comparable age (Figs. S8A and B). Furthermore, progranulin was not found to be increased in the hippocampus or striatum of *Shank3* KO mice (Figs. S8C and D). Therefore, increased progranulin expression in early adulthood is not necessary for the manifestation of autistic-like phenotypes in mice.

Having shown that increased progranulin expression is neither necessary nor sufficient to cause autistic-like phenotypes in mice, we next evaluated whether a genetic reduction of progranulin expression could ameliorate the FXS-associated phenotypes in *Fmr1* KO mice. Zhang et al. (2017) demonstrated that a targeted reduction of progranulin expression by lentiviral transduction of progranulin-specific shRNA could reverse multiple behavioural and synaptic phenotypes in *Fmr1* KO mice (Zhang et al., 2017). We hypothesized that a genetic reduction of progranulin in *Fmr1* KO mice would be sufficient to abrogate FXS-associated physiological, behavioural, and biochemical

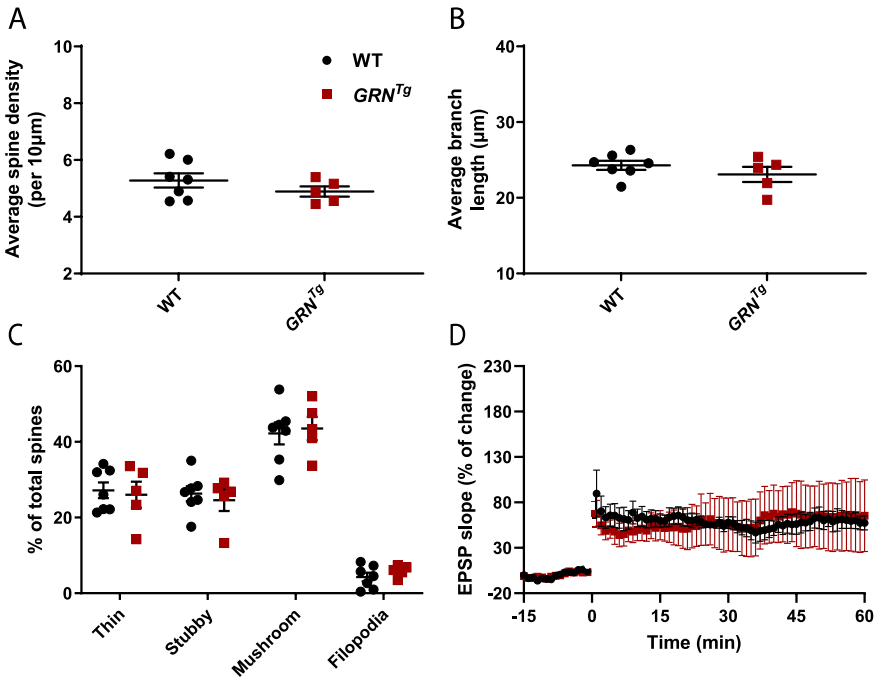

Fig. 4. Genetic over-expression of progranulin throughout development does not cause changes to dendritic spine density, dendritic spine morphology, or long-term potentiation in the CA1. Golgi cox staining was performed on n = 7 wild-type (black) and n = 5 GRN^{Tg} (red) male mice at postnatal day 13. Spine density (A), branch length (B), and spine morphology (C) are evaluated in the CA1. D) Long-term potentiation was assessed in n = 4 hippocampal slices from two WT mice and n = 4 hippocampal slices from three GRN^{Tg} mice. Field excitatory postsynaptic potentials were measured every minute for 15 min prior to high frequency stimulation after which responses were recorded for an additional 60 min. Data are presented as mean ± standard error of the mean (SEM). Data are analyzed by unpaired *t*-test for A and B and two-way ANOVA with Šídák's multiple comparisons test for genotype effects for C. No significant difference is observed in any comparison. (For interpretation of the references to colour in this figure legend, the reader is referred to the Web version of this article.)

phenotypes. To assess this hypothesis, we bred male *Fmr1*+; $Grn^{+/-}$ and female $Fmr1^{+/-}$; $Grn^{+/+}$ mice to generate male littermates of the following genotypes 1) *Fmr1*+; $Grn^{+/+}$ 2) *Fmr1*+; $Grn^{+/-}$ 3) *Fmr1* KO; $Grn^{+/+}$ and 4) *Fmr1* KO; $Grn^{+/-}$. We first confirmed that mice with the $Grn^{+/-}$ genetic background express 50% less progranulin protein than $Grn^{+/+}$ mice by performing an ELISA on cortical lysate (Fig. S9). We subsequently determined that FMRP is not expressed in *Fmr1* KO mouse cortical lysate at detectable levels by western blot (Fig. S10).

After validating the strains, we endeavoured to characterize the effect of a genetic reduction of progranulin expression on *Fmr1* KO mouse behaviour and physiology. No differences were observed in 2-month body weight in male *Fmr1*+; $Grn^{+/+}$, *Fmr1* KO; $Grn^{+/+}$, *Fmr1* KO; $Grn^{+/-}$, and *Fmr1*+; $Grn^{+/-}$ mice (Fig. 5A). We then evaluated hyperactivity in the aforementioned strains in the open field test (Fig. 5B). The absence of *Fmr1* expression was observed to cause hyperactivity, but progranulin gene dosage had no effect on this phenomenon (Fig. 5B). Similarly, *Fmr1* KO mice exhibited significantly reduced anxiety behaviour in the elevated plus maze, but loss of one copy of progranulin expression did not modify this phenotype (Fig. 5C). No genotypic differences in repetitive behaviour engagement or sociability were observed in any strain as assessed by marble burying and the three-chamber test, respectively (Fig. 5D, Fig. S11). While testes weight was significantly increased in *Fmr1* KO mice as expected, we noted that testes weight was qualitatively decreased in *Fmr1* KO; $Grn^{+/-}$ mice as compared to *Fmr1* KO; $Grn^{+/+}$ mice (Fig. 5E). Progranulin gene dosage itself was not a significant predictor of testes weight but the interaction between progranulin dosage and *Fmr1* dosage was significant (Fig. 5E). This suggests that progranulin is implicated in the development macroorchidism in *Fmr1* KO mice.

While loss of one copy of progranulin had little effect on autistic-like behaviour in *Fmr1* KO mice, we proceeded to probe for modification of biochemical phenotypes. *Fmr1* KO mice have been previously observed to exhibit increased activation in the MAPK/ERK pathway which is thought to contribute to the increased expression of several proteins, including MMP9 (Sawicka et al., 2016; Wang et al., 2012; Bilousova et al., 2009). To this end, we first evaluated ERK expression by western blot in cortical lysate from n = 8 3-month-old wild-type (*Fmr1*+; $Grn^{+/+}$) and *Fmr1* KO; $Grn^{+/+}$ mice. ERK expression in the *Fmr1* KO mice was found to be indistinguishable from wild-type mice (Fig. 6A and B). Similarly, *Fmr1* dosage was not found to modify pERK levels (Fig. 6C and D), the ratio of pERK to ERK (Fig. 6E), or MMP9 expression (Fig. 6F and G). In a subsequent pairwise comparison, we sought to determine the effect of reduced progranulin expression on an *Fmr1* KO background on the MAPK/ERK pathway. *Fmr1* KO; $Grn^{+/-}$ mice did not express cortical ERK at levels significantly different than *Fmr1* KO; $Grn^{+/+}$ mice (Fig. 7A and B). No differences in pERK levels were observed in these strains (Fig. 7C and D). Additionally, the ratio of pERK to ERK and MMP9 expression were not modified by genetic reduction of progranulin expression (Fig. 7E–G). In sum, we find no phenotypic changes to the cortical MAPK/ERK pathway caused by loss of *Fmr1*, nor modification of this pathway in *Fmr1* KO; $Grn^{+/-}$ mice.

4. Discussion

Here we report the characterization of progranulin expression in *Fmr1* KO mice. Zhang et al. (2017) previously identified increased progranulin mRNA and protein expression in the prefrontal cortex of *Fmr1* KO mice, with no change in progranulin expression in the hippocampus (Zhang et al., 2017). We corroborate these findings with the exception that no increase in progranulin mRNA was detected in the prefrontal cortex, or in any tissue evaluated (Fig. S2). We have extended these finding to report that progranulin protein is upregulated post-transcriptionally in the *Fmr1* KO prefrontal cortex, brainstem, liver, and lung (Fig. 1, Fig. S2). Further, we identified an association between FMRP and progranulin mRNA by RNA immunoprecipitation (Fig. 2). An interaction between FMRP and progranulin mRNA has been implied by previous large scale FMRP crosslinked immunoprecipitation experiments but this interaction did not reach significance in any case (Darnell et al., 2011; Ascano et al., 2012; Maurin et al., 2018). We propose that the significance of the FMRP-progranulin mRNA interaction observed in the present work is due in part to the targeted nature of the query (reducing the false discovery rate threshold) and in part to methodological differences (no crosslinking was used in this study). Nevertheless, an interaction between progranulin mRNA and FMRP suggests that progranulin is upregulated in *Fmr1* KO mice because progranulin is an FMRP target. Why progranulin protein expression is upregulated in some tissues but not others is a question of interest for further study.

After observing upregulated progranulin expression in *Fmr1* KO

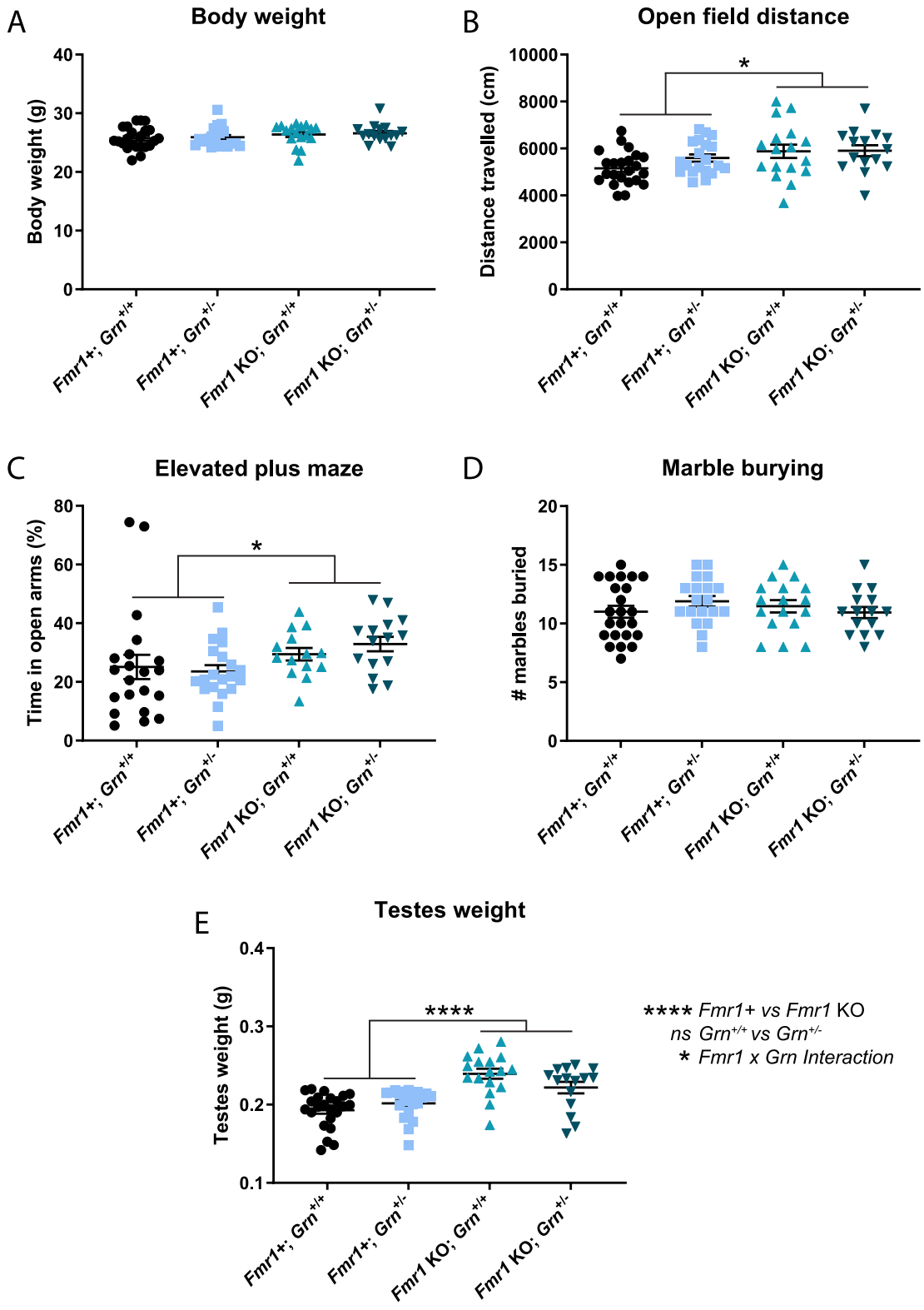

Fig. 5. Genetic reduction of progranulin expression reduces macroorchidism in *Fmr1* KO mice without modifying FXS-associated behavioural phenotypes. Body weight (A), behaviour (B–D) and testes weight (E) are characterized in n = 23 wild type (*Fmr1+; Grn*$^{+/+}$), n = 20 *Fmr1+; Grn*$^{+/-}$, n = 17 *Fmr1* KO*; Grn*$^{+/+}$, and n = 15 *Fmr1* KO*; Grn*$^{+/-}$ male mice, aged 2–3 months. Activity in open field is measured in (B), while the results of the elevated plus maze and marble burying are shown in (C) and (D) respectively. Testes weight (E) is given as the combined weight of both testes from a single individual. Data are presented as mean ± standard error of the mean (SEM). Data are analyzed by two-way ANOVA for *Fmr1* and *Grn* gene dosage. Šídák's multiple comparisons test was conducted between the *Fmr1* KO*; Grn*$^{+/+}$ and *Fmr1* KO*; Grn*$^{+/-}$ genotypes to assess whether progranulin reduction could modify FXS-associated phenotypes on an *Fmr1* KO background. *p < 0.05 by two-way ANOVA, ****p < 0.0001 by two-way ANOVA, ns not significant.

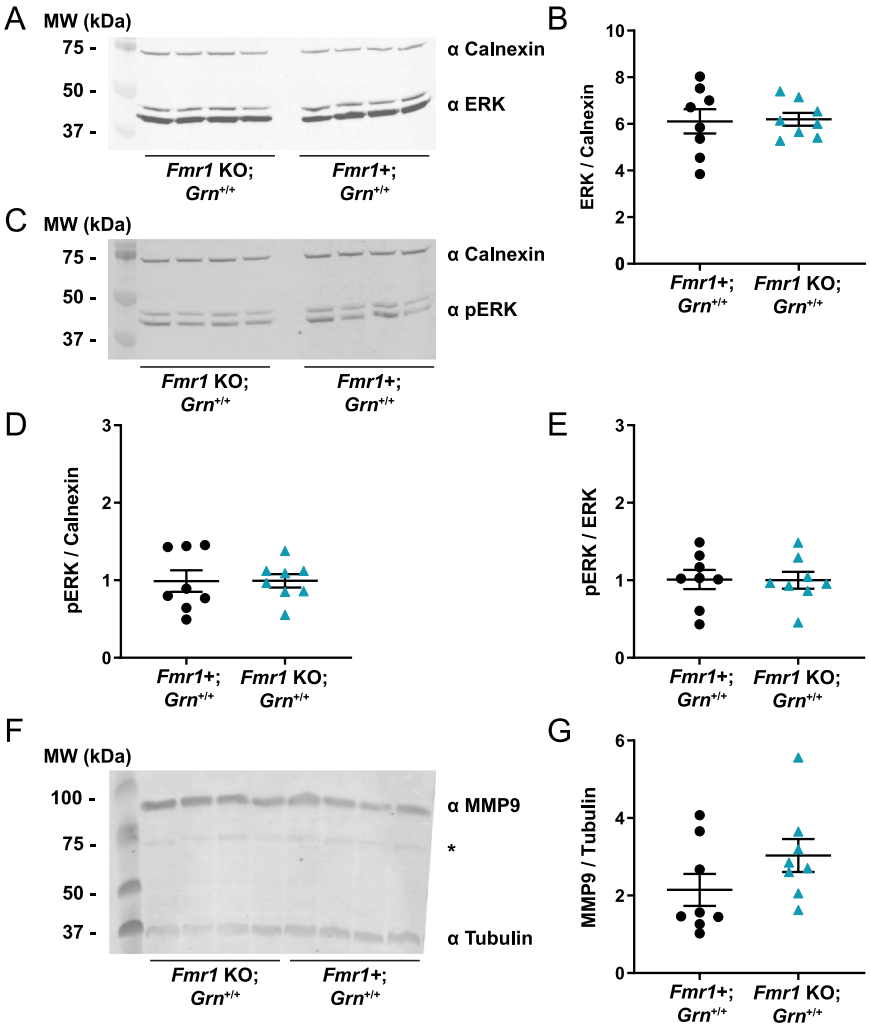

Fig. 6. Loss of *Fmr1* expression in mice does not modify cortical ERK, pERK, or MMP9 expression. Cortical ERK expression is evaluated by western blot in n = 8 wild-type (*Fmr1+; Grn*$^{+/+}$; black circles) and n = 8 *Fmr1* KO (*Fmr1* KO; *Grn*$^{+/+}$; teal triangles) male mice at 3 months of age (A,B). Similarly, pERK expression and the pERK/ERK ratio are evaluated in the same samples in (C,D) and (E), respectively. MMP9 expression is shown in (F,G). ERK and pERK are normalized to calnexin, while MMP9 expression is normalized to β-tubulin. Cortical lysate input is normalized to 30ug total protein by Bradford assay. Data are presented as mean ± standard error of the mean (SEM). Data are analyzed by unpaired *t*-test. No significant difference is observed in any comparison.

mice, we sought to determine if constitutive progranulin over-expression is sufficient to phenocopy FXS-associated endpoints in mice. Genetic over-expression of progranulin on an *Fmr1+* background had modest effects on autism-associated behaviours (Fig. 3, Fig. S3, Fig. S4). Of note, progranulin over-expressing females exhibited reduced repetitive behaviour engagement in the marble burying test (Fig. S4D) and males demonstrated subtle hyperactivity (Fig. S3). While hyperactivity is consistent with FXS-associated behaviour in *Fmr1* KO mice (The Dutch-Belgian Fragile et al., 1994; Liu et al., 2011; Ding et al., 2014), a prior study has reported increased repetitive behaviour engagement in *Fmr1* KO female mice (Gholizadeh et al., 2014), suggesting that constitutive progranulin over-expression is capable of modifying mouse behaviour by mechanisms independent from those associated with FXS.

In an effort to better understand the neurophysiological origin of these behavioural phenotypes, we characterized dendritic spine morphology in *GRN*^{Tg} mice, again using FXS-associated endpoints as a guide. While relative immaturity of dendritic spines has been observed in two-week-old *Fmr1* KO cortex layer V neurons (Nimchinsky et al., 2001; Su et al., 2011), we observed no changes to spine maturity in the cortical layer V neurons of *GRN*^{Tg} mice at this time point (Fig. S6). Similarly, reduced spine maturity has been observed in *Fmr1* KO CA1 pyramidal neurons at one week of age (Bilousova et al., 2009), and we report normal spine maturity in these neurons in *GRN*^{Tg} mice at two weeks of age (Fig. 4). Abnormal spine density has also been described in these regions in *Fmr1* KO mice (Reviewed in (He and Portera-Cailliau, 2013)) but we identified no abnormality in *GRN*^{Tg} dendritic spine density in the regions evaluated (Fig. 4, Fig. S6). The absence of detectable changes to spine density and morphology in *GRN*^{Tg} mice is supported by our electrophysiological data. Indeed, no differences in LTP were observed in the CA1 or dentate gyrus of *GRN*^{Tg} mice (Fig. 4D, Fig. S7). These findings suggest that mouse hippocampal neurophysiology is resilient to increased progranulin expression. Hence, we may expect that progranulin dysregulation is not a direct effector in the FXS-associated hippocampal neurophysiological phenotypes (Bilousova et al., 2009; He and Portera-Cailliau, 2013) observed in *Fmr1* KO mice. In this context, it is noteworthy that progranulin expression does not appear to vary between wild-type and *Fmr1* KO mouse hippocampi (Fig. 1A). (Zhang et al., 2017)

Based on previous work reporting that targeted reduction of progranulin expression was sufficient to ameliorate FXS-like behaviour and physiology in *Fmr1* KO mice (Zhang et al., 2017), we tested whether genetic reduction of progranulin expression would be protective against the development of these phenotypes in *Fmr1* KO mice. We found that decreased progranulin expression due to deletion of a single copy of the progranulin gene had no effect on the autism-associated open field hyperactivity or elevated plus maze anxiety deficits in *Fmr1* KO mice (Fig. 5B and C). However, reduced progranulin expression did partially ameliorate FXS-associated macroorchidism in *Fmr1* KO; *Grn*$^{+/-}$ mice (Fig. 5E).

Macroorchidism in FXS is thought to be caused by increased

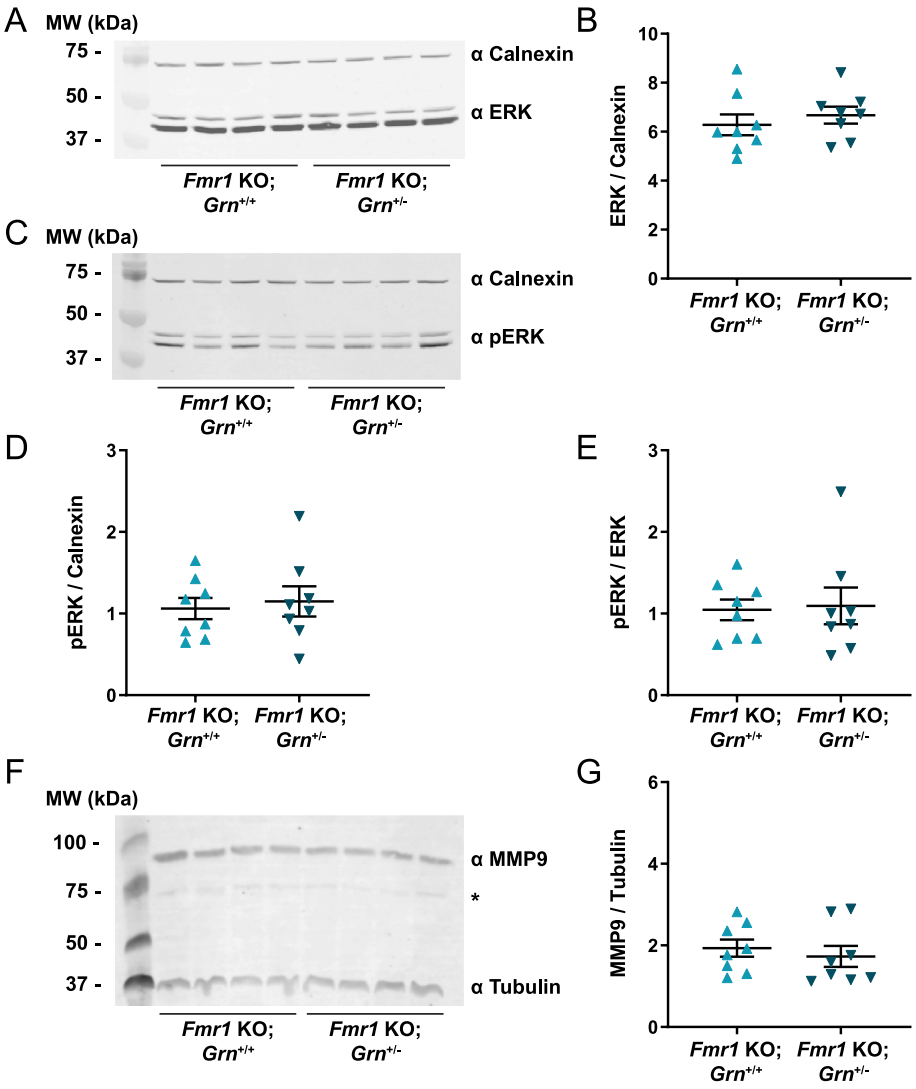

Fig. 7. Genetic reduction of progranulin expression does not modify cortical ERK, pERK, or MMP9 expression on an *Fmr1* KO background. Cortical ERK expression is evaluated by western blot in n = 8 *Fmr1* KO; $Grn^{+/+}$ (teal triangles) and n = 8 *Fmr1* KO; $Grn^{+/-}$ (dark blue inverted triangles) male mice at 3 months of age (A,B). Similarly, pERK expression and the pERK/ERK ratio are evaluated in the same samples in (C,D) and (E), respectively. MMP9 expression is shown in (F,G). ERK and pERK are normalized to calnexin, while MMP9 expression is normalized to β-tubulin. Cortical lysate input is normalized to 30ug total protein by Bradford assay. Data are presented as mean ± standard error of the mean (SEM). Data are analyzed by unpaired *t*-test. No significant difference is observed in any comparison. (For interpretation of the references to colour in this figure legend, the reader is referred to the Web version of this article.)

proliferation of Sertoli cells (Slegtenhorst-Eegdeman et al., 1998). Both FMRP and progranulin are expressed in Sertoli cells (Daniel et al., 2000; Bakker et al., 2000) and have been shown to regulate cell proliferation (Zanocco-Marani et al., 1999; Xu et al., 1998; Luo et al., 2010). To our knowledge, the extent of overlap between the two mechanisms of cell proliferation regulation has never been studied. However, it is notable that both FMRP and progranulin have been observed to modify Wnt signalling (de la Encarnación et al., 2016; Rosen et al., 2011; Pedini et al., 2022), a fundamental pathway in embryonic development, apoptosis, and cellular proliferation (reviewed in Teo and Kahn (2010)). While a complete interrogation of the role of progranulin in Sertoli cell proliferation is beyond the scope of this study, our data suggests that there exists some overlap in the mechanisms by which FMRP and progranulin regulate Sertoli cell proliferation, perhaps through Wnt signalling or an alternative pathway. We propose that the mechanistic overlap is indirect given that testicular progranulin expression is not upregulated in the absence of FMRP (Fig. 1B). We also note that increased progranulin expression alone is not sufficient to cause macroorchidism because GRN^{Tg} mice were observed to have normal testes weights (Fig. S5).

Further interrogation of progranulin's role in FXS-associated macroorchidism may benefit from the inclusion of a metformin treatment group. Metformin is emerging as a promising therapeutic for FXS (Gantois et al., 2017, 2019; Protic et al., 2019a, 2019b; Biag et al., 2019), and clinical trials are ongoing (Dy et al., 2018; Proteau-Lemieux et al., 2021). Metformin treatment has been found to ameliorate several FXS-associated symptoms in mice, including macroorchidism (Gantois et al., 2017). Metformin has diverse effects, having been found to modify cell proliferation, apoptosis (Xiong et al., 2019; Griss et al., 2015), and regulate Wnt signalling through AMP-activated protein kinase (AMPK) dependent (Park et al., 2019) and AMPK-independent mechanisms (Conza et al., 2021). Additionally, it is worth noting that metformin treatment has appears to have therapeutic utility in the context of diabetes, cancer, and FXS (reviewed in (Gantois et al., 2019; Drzewoski and Hanefeld, 2021)). Progranulin overexpression has been implicated in each of these conditions (Zhang et al., 2017; Nicoletto and Canani, 2015; Arechavaleta-Velasco et al., 2017), suggesting that further study into the progranulin/metformin axis may yield insights into common pathological mechanisms.

One limitation of the research presented herein is the lack of robust autism-associated phenotypes observed in the *Fmr1* KO mice. We detected FXS-associated behavioural phenotypes in open field and elevated plus maze, though they were subtle and only significant when the *Fmr1* KO; $Grn^{+/+}$ and *Fmr1* KO; $Grn^{+/-}$ mice groups were aggregated (Fig. 5). The previously reported *Fmr1* KO associated hyperactivation of the MAPK/ERK pathway (Sidhu et al., 2014; Wen et al., 2018; Sawicka et al., 2016; Wang et al., 2012) was not observed in our mice (Fig. 6), complicating our ability to assess the effect of progranulin reduction on

this endpoint. The partial alignment of observed phenotypes in *Fmr1* KO mice is consistent with the substantial discordance of reported phenotypes in this strain (Kazdoba et al., 2014). Indeed, such discordance has been described as reflective of the clinical heterogeneity of patients with FXS (Kazdoba et al., 2014). While a complete explanation for the subtlety of *Fmr1* KO phenotypes observed in the present study is lacking, we note that the *Fmr1* KO mice were generated with wild-type littermates. Though this breeding scheme reduces variability and improves genotypic blinding for researchers, it also gives the *Fmr1* KO mice abundant access to interaction with behaviourally normal mice. As behavioural intervention is a leading treatment for autism (Lovaas, 1987; Eldevik et al., 2009), we suggest that exposure to wild-type animals may have reduced the extent of autism-associated phenotypes in *Fmr1* KO mice. Future studies seeking to evaluate the effect of genetic modification on an *Fmr1* KO background may benefit from breeding *Fmr1* KO mice separately or exacerbating the autism-associated phenotypes with an additional autism risk factor, such as postpartum maternal separation or *in utero* valproic acid exposure (VPA) (Petroni et al., 2022; Yang et al., 2016).

Our data suggest that constitutive over-expression of progranulin expression does not significantly modify symptom severity or risk of developing autism in mice. However, we cannot at this time rule out increased progranulin expression as a risk factor for the development of autism. We were unable to evaluate the effect of genetic over-expression of progranulin on the autistic-like phenotypes in *Fmr1* KO mice in this work because *Fmr1* and *Hprt* (the transgene locus) are within 8 centimorgans (Davisson et al., 1998), such that the generation of *Fmr1* KO; GRN^{Tg} mice would require an extensive breeding program beyond the scope of this study. Nevertheless, the minimal effects of a genetic reduction of progranulin expression on *Fmr1* KO phenotypes and the mildness of phenotypes in progranulin over-expressing mice suggests that genetic under- or over-expression of progranulin is not a significant contributor to autism risk in mice. Instead, progranulin's role in the development of autism may be more complex, involving tissue-specific progranulin dysregulation at critical timepoints.

A causative role for acute, localized upregulation of progranulin expression in the development of autism would be parsimonious given the number of environmental risk factors for autism that engender increased progranulin levels. Several autism-associated environmental risk factors have received supporting evidence, including gestational diabetes mellitus, maternal obesity, neonatal hypoxia, VPA exposure, advanced parental age, and preterm birth (Lord et al., 2020). Many of these can be linked, at least correlatively, to increased progranulin expression. Patients with diabetes have previously been shown to exhibit an enrichment in serum progranulin expression, a phenomenon that correlates significantly with BMI (Youn et al., 2009; Qu et al., 2013; Hossein-Nezhad et al., 2012). Hypoxic conditions induced progranulin upregulation in both human neuroblastomas and rat fibroblasts (Piscopo et al., 2010; Guerra et al., 2007). Moreover, perinatal exposure to hypoxia caused the upregulation of progranulin mRNA in newborn rat cortices (Piscopo et al., 2016). VPA treatment of human iPSC-derived neural progenitor cells and neurons has similarly been found to increase progranulin expression (She et al., 2017). The effects of VPA on progranulin expression during development have been further characterized in rodents.

VPA exposure *in utero* has been shown to induce dysregulated progranulin expression during development and implicated this dysregulation in autism pathology. In a recent study, VPA injection during pregnancy was found to modify autism-associated repetitive behaviour in rats (Lan et al., 2021). This VPA exposure also altered progranulin expression in a time-dependent and subregion-specific manner. Specifically, VPA induced a transient increase in progranulin expression in the prefrontal cortex from 2 to 5 weeks postnatal and reduced hippocampal progranulin expression from 5 to 10 weeks (Lan et al., 2021). These changes in progranulin expression correlated with changes in apoptotic protein expression, neuronal number, dendritic spine density, and synaptic protein levels (Lan et al., 2021). A follow-up study from the same group demonstrated that direct injection of recombinant human progranulin into the cerebellum of VPA-exposed rat pups was sufficient to ameliorate synaptic, apoptotic, and behavioural phenotypes (Wang et al., 2022). These studies imply that tissue-specific and time-specific progranulin dysregulation is of pathological relevance in VPA-associated autism.

Aberrant progranulin expression in the brain has now been observed by multiple groups in at least two rodent models of autism (*Fmr1* KO mice and *in utero* VPA exposure). In this work, we demonstrated that progranulin is upregulated in 2-month-old *Fmr1* KO mice in a manner that is both post-transcriptional and tissue-specific (Fig. 1, Fig. S1, Fig. S2). Spatial and temporal dysregulation of progranulin expression has been observed in the brains of *Fmr1* KO mice and VPA-exposed rats (Zhang et al., 2017; Lan et al., 2021). Considering this data and the observed subtle effects of genetic modification of progranulin expression on autistic-like phenotypes described herein, we suggest that acute spatial and temporal dysregulation of progranulin expression during development is more likely to be of pathological significance in autism than global up or down-regulation of progranulin. How exactly this regional and subregional dysregulation of progranulin expression modifies autism risk remains a worthy area of study, capable of informing both progranulin biology and autism pathophysiology.

Ethics approval

All animal work was approved by the UBC Animal Care Committee and the Canadian Council on Animal Care.

Consent for publication

All authors have read and approved this manuscript for publication.

Availability of data and material

Descriptive statistics for all figures can be found in Supplementary Table 3 and Supplementary Table 4. All numerical data is included in the Supplementary Material and is separated by figure.

Funding

This work was partially supported by the British Columbia Children's Hospital Research Institute's Brain, Behaviour and Development research theme.

Author's contributions

BL and BRL conceived of the research project. BL designed, performed, and analyzed the following experiments: ELISAs, RNA immunoprecipitations, western blots, qPCRs, Golgi-cox, and mouse behaviour studies. LB and BC designed the electrophysiology experiments, with LB performing and analyzing this work. IG provided the *Shank3* KO tissue and contributed to the design of the experiment in which this tissue was used. BL wrote this manuscript, with edits from LB, IG, BC, and BRL.

CRediT authorship contribution statement

Benjamin Life: Conceptualization, Validation, Formal analysis, Investigation, Visualization, Writing – original draft. **Luis E.B. Bettio:** Formal analysis, Investigation, Writing – review & editing. **Ilse Gantois:** Resources, Writing – review & editing. **Brian R. Christie:** Resources, Supervision, Writing – review & editing. **Blair R. Leavitt:** Conceptualization, Supervision, Writing – review & editing.

Declaration of competing interest

The authors declare that they have no known competing financial interests or personal relationships that could have appeared to influence the work reported in this paper.

Data availability

Data will be made available on request.

Acknowledgements

The authors would like to thank Ge Lu and Alissandra de Moura Gomes for their technical expertise in collecting tissue from *Fmr1* KO and wild-type mice. We are also grateful to Dr. Terri Petkau for developing the Golgi-cox protocol used in this manuscript.

Appendix A. Peer Review Overview and Supplementary data A Peer Review Overview

Supplementary data to this article can be found online at https://doi.org/10.1016/j.crneur.2023.100094.

References

Arechavaleta-Velasco, F., Perez-Juarez, C.E., Gerton, G.L., Diaz-Cueto, L., 2017. Progranulin and its biological effects in cancer. Med. Oncol. 34, 194.
Ascano Jr., M., Mukherjee, N., Bandaru, P., Miller, J.B., Nusbaum, J.D., Corcoran, D.L., Langlois, C., Munschauer, M., Dewell, S., Hafner, M., et al., 2012. FMRP targets distinct mRNA sequence elements to regulate protein expression. Nature 492, 382–386.
Ashley Jr., C.T., Wilkinson, K.D., Reines, D., Warren, S.T., 1993. FMR1 protein: conserved RNP family domains and selective RNA binding. Science 262, 563–566.
Baio, J., Wiggins, L., Christensen, D.L., Maenner, M.J., Daniels, J., Warren, Z., Kurzius-Spencer, M., Zahorodny, W., Robinson Rosenberg, C., White, T., et al., 2018. Prevalence of autism spectrum disorder among children aged 8 Years - autism and developmental disabilities monitoring network, 11 sites, United States, 2014. MMWR Surveill Summ. 67, 1–23.
Baker, M., Mackenzie, I.R., Pickering-Brown, S.M., Gass, J., Rademakers, R., Lindholm, C., Snowden, J., Adamson, J., Sadovnick, A.D., Rollinson, S., et al., 2006. Mutations in progranulin cause tau-negative frontotemporal dementia linked to chromosome 17. Nature 442, 916–919.
Bakker, C.E., de Diego Otero, Y., Bontekoe, C., Raghoe, P., Luteijn, T., Hoogeveen, A.T., Oostra, B.A., Willemsen, R., 2000. Immunocytochemical and biochemical characterization of FMRP, FXR1P, and FXR2P in the mouse. Exp. Cell Res. 258, 162–170.
Baxter, A.J., Brugha, T.S., Erskine, H.E., Scheurer, R.W., Vos, T., Scott, J.G., 2015. The epidemiology and global burden of autism spectrum disorders. Psychol. Med. 45, 601–613.
Biag, H.M.B., Potter, L.A., Wilkins, V., Afzal, S., Rosvall, A., Salcedo-Arellano, M.J., Rajaratnam, A., Manzano-Nunez, R., Schneider, A., Tassone, F., et al., 2019. Metformin treatment in young children with fragile X syndrome. Mol. Genet. Genom. Med. 7, e956.
Bilousova, T.V., Dansie, L., Ngo, M., Aye, J., Charles, J.R., Ethell, D.W., Ethell, I.M., 2009. Minocycline promotes dendritic spine maturation and improves behavioural performance in the fragile X mouse model. J. Med. Genet. 46, 94.
Bostrom, C.A., Majaess, N.M., Morch, K., White, E., Eadie, B.D., Christie, B.R., 2015. Rescue of NMDAR-dependent synaptic plasticity in Fmr1 knock-out mice. Cerebr. Cortex 25, 271–279.
Coffee, B., Zhang, F., Warren, S.T., Reines, D., 1999. Acetylated histones are associated with FMR1 in normal but not fragile X-syndrome cells. Nat. Genet. 22, 98–101.
Coffee, B., Zhang, F., Ceman, S., Warren, S.T., Reines, D., 2002. Histone modifications depict an aberrantly heterochromatinized FMR1 gene in fragile x syndrome. Am. J. Hum. Genet. 71, 923–932.
Conza, D., Mirra, P., Calì, G., Insabato, L., Fiory, F., Beguinot, F., Ulianich, L., 2021. Metformin dysregulates the unfolded protein response and the WNT/β-Catenin pathway in endometrial cancer cells through an AMPK-independent mechanism. Cells 10.
Cruts, M., Gijselinck, I., van der Zee, J., Engelborghs, S., Wils, H., Pirici, D., Rademakers, R., Vandenberghe, R., Dermaut, B., Martin, J.J., et al., 2006. Null mutations in progranulin cause ubiquitin-positive frontotemporal dementia linked to chromosome 17q21. Nature 442, 920–924.
Daniel, R., He, Z., Carmichael, K.P., Halper, J., Bateman, A., 2000. Cellular localization of gene expression for progranulin. J. Histochem. Cytochem. 48, 999–1009.
Darnell, J.C., Van Driesche, S.J., Zhang, C., Hung, K.Y., Mele, A., Fraser, C.E., Stone, E.F., Chen, C., Fak, J.J., Chi, S.W., et al., 2011. FMRP stalls ribosomal translocation on mRNAs linked to synaptic function and autism. Cell 146, 247–261.
Davis, J.K., Broadie, K., 2017. Multifarious functions of the fragile X mental retardation protein. Trends Genet. 33, 703–714.
Davisson, M.T., Bradt, D.W., Merriam, J.J., Rockwood, S.F., Eppig, J.T., 1998. The mouse gene Map. ILAR J. 39, 96–131.
de la Encarnación, A., Alquézar, C., Martín-Requero Á, 2016. Increased Wnt signaling and reduced viability in a neuronal model of progranulin-deficient frontotemporal lobar degeneration. Mol. Neurobiol. 53, 7107–7118.
Ding, Q., Sethna, F., Wang, H., 2014. Behavioral analysis of male and female Fmr1 knockout mice on C57BL/6 background. Behav. Brain Res. 271, 72–78.
Drzewoski, J., Hanefeld, M., 2021. The current and potential therapeutic use of metformin-the good old drug. Pharmaceuticals 14.
Durand, C.M., Betancur, C., Boeckers, T.M., Bockmann, J., Chaste, P., Fauchereau, F., Nygren, G., Rastam, M., Gillberg, I.C., Anckarsäter, H., et al., 2007. Mutations in the gene encoding the synaptic scaffolding protein SHANK3 are associated with autism spectrum disorders. Nat. Genet. 39, 25–27.
Dy, A.B.C., Tassone, F., Eldeeb, M., Salcedo-Arellano, M.J., Tartaglia, N., Hagerman, R., 2018. Metformin as targeted treatment in fragile X syndrome. Clin. Genet. 93, 216–222.
Eadie, B.D., Cushman, J., Kannangara, T.S., Fanselow, M.S., Christie, B.R., 2012. NMDA receptor hypofunction in the dentate gyrus and impaired context discrimination in adult Fmr1 knockout mice. Hippocampus 22, 241–254.
Eldevik, S., Hastings, R.P., Hughes, J.C., Jahr, E., Eikeseth, S., Cross, S., 2009. Meta-analysis of early intensive behavioral intervention for children with autism. J. Clin. Child Adolesc. Psychol. 38, 439–450.
Elia, L.P., Mason, A.R., Alijagic, A., Finkbeiner, S., 2019. Genetic regulation of neuronal progranulin reveals a critical role for the autophagy-lysosome pathway. J. Neurosci. 39, 3332.
Gantois, I., Khoutorsky, A., Popic, J., Aguilar-Valles, A., Freemantle, E., Cao, R., Sharma, V., Pooters, T., Nagpal, A., Skalecka, A., et al., 2017. Metformin ameliorates core deficits in a mouse model of fragile X syndrome. Nat. Med. 23, 674–677.
Gantois, I., Popic, J., Khoutorsky, A., Sonenberg, N., 2019. Metformin for treatment of fragile X syndrome and other neurological disorders. Annu. Rev. Med. 70, 167–181.
Gauthier, J., Spiegelman, D., Piton, A., Lafrenière, R.G., Laurent, S., St-Onge, J., Lapointe, L., Hamdan, F.F., Cossette, P., Mottron, L., et al., 2009. Novel de novo SHANK3 mutation in autistic patients. Am. J. Med. Genet. B Neuropsychiatr. Genet. 150b, 421–424.
Gholizadeh, S., Arsenault, J., Xuan, I.C., Pacey, L.K., Hampson, D.R., 2014. Reduced phenotypic severity following adeno-associated virus-mediated Fmr1 gene delivery in fragile X mice. Neuropsychopharmacology 39, 3100–3111.
Griss, T., Vincent, E.E., Egnatchik, R., Chen, J., Ma, E.H., Faubert, B., Viollet, B., DeBerardinis, R.J., Jones, R.G., 2015. Metformin antagonizes cancer cell proliferation by suppressing mitochondrial-dependent biosynthesis. PLoS Biol. 13, e1002309.
Guerra, R.R., Kriazhev, L., Hernandez-Blazquez, F.J., Bateman, A., 2007. Progranulin is a stress-response factor in fibroblasts subjected to hypoxia and acidosis. Growth Factors 25, 280–285.
He, C.X., Portera-Cailliau, C., 2013. The trouble with spines in fragile X syndrome: density, maturity and plasticity. Neuroscience 251, 120–128.
Hébert, B., Pietropaolo, S., Même, S., Laudier, B., Laugeray, A., Doisne, N., Quartier, A., Lefeuvre, S., Got, L., Cahard, D., et al., 2014. Rescue of fragile X syndrome phenotypes in Fmr1KO mice by a BKCa channel opener molecule. Orphanet J. Rare Dis. 9, 124.
Heulens, I., D'Hulst, C., Van Dam, D., De Deyn, P.P., Kooy, R.F., 2012. Pharmacological treatment of fragile X syndrome with GABAergic drugs in a knockout mouse model. Behav. Brain Res. 229, 244–249.
Hinton, V.J., Brown, W.T., Wisniewski, K., Rudelli, R.D., 1991. Analysis of neocortex in three males with the fragile X syndrome. Am. J. Med. Genet. 41, 289–294.
Hossein-Nezhad, A., Mirzaei, K., Ansar, H., Emam-Gholipour, S., Tootee, A., Keshavarz, S.A., 2012. Obesity, inflammation and resting energy expenditure: possible mechanism of progranulin in this pathway. Minerva Endocrinol. 37, 255–266.
Huber, K.M., Gallagher, S.M., Warren, S.T., Bear, M.F., 2002. Altered synaptic plasticity in a mouse model of fragile X mental retardation. Proc. Natl. Acad. Sci. U. S. A 99, 7746–7750.
Hunter, J., Rivero-Arias, O., Angelov, A., Kim, E., Fotheringham, I., Leal, J., 2014. Epidemiology of fragile X syndrome: a systematic review and meta-analysis. Am. J. Med. Genet. 164, 1648–1658.
Irwin, S.A., Patel, B., Idupulapati, M., Harris, J.B., Crisostomo, R.A., Larsen, B.P., Kooy, F., Willems, P.J., Cras, P., Kozlowski, P.B., et al., 2001. Abnormal dendritic spine characteristics in the temporal and visual cortices of patients with fragile-X syndrome: a quantitative examination. Am. J. Med. Genet. 98, 161–167.
Kamate, M., Detroja, M., Hattiholi, V., 2019. Neuronal ceroid lipofuscinosis type-11 in an adolescent. Brain Dev. 41, 542–545.
Kazdoba, T.M., Leach, P.T., Silverman, J.L., Crawley, J.N., 2014. Modeling fragile X syndrome in the Fmr1 knockout mouse. Intractable Rare Dis. Res. 3, 118–133.
Lachiewicz, A.M., Dawson, D.V., 1994. Do young boys with fragile X syndrome have macroorchidism? Pediatrics 93, 992–995.
Laggerbauer, B., Ostareck, D., Keidel, E.M., Ostareck-Lederer, A., Fischer, U., 2001. Evidence that fragile X mental retardation protein is a negative regulator of translation. Hum. Mol. Genet. 10, 329–338.
Laird, A.S., Van Hoecke, A., De Muynck, L., Timmers, M., Van den Bosch, L., Van Damme, P., Robberecht, W., 2010. Progranulin is neurotrophic in vivo and protects against a mutant TDP-43 induced axonopathy. PLoS One 5, e13368.
Lan, J., Hu, Y., Wang, X., Zheng, W., Liao, A., Wang, S., Li, Y., Wang, Y., Yang, F., Chen, D., 2021. Abnormal spatiotemporal expression pattern of progranulin and

neurodevelopment impairment in VPA-induced ASD rat model. Neuropharmacology 196, 108689.
Li, Z., Zhang, Y., Ku, L., Wilkinson, K.D., Warren, S.T., Feng, Y., 2001. The fragile X mental retardation protein inhibits translation via interacting with mRNA. Nucleic Acids Res. 29, 2276–2283.
Li, J., Pelletier, M.R., Perez Velazquez, J.L., Carlen, P.L., 2002. Reduced cortical synaptic plasticity and GluR1 expression associated with fragile X mental retardation protein deficiency. Mol. Cell. Neurosci. 19, 138–151.
Liu, Z.H., Chuang, D.M., Smith, C.B., 2011. Lithium ameliorates phenotypic deficits in a mouse model of fragile X syndrome. Int. J. Neuropsychopharmacol. 14, 618–630.
Lord, C., Brugha, T.S., Charman, T., Cusack, J., Dumas, G., Frazier, T., Jones, E.J.H., Jones, R.M., Pickles, A., State, M.W., et al., 2020. Autism spectrum disorder. Nat. Rev. Dis. Prim. 6, 5.
Lovaas, O.I., 1987. Behavioral treatment and normal educational and intellectual functioning in young autistic children. J. Consult. Clin. Psychol. 55, 3–9.
Lpjj, Noldus, Spink, A.J., Tegelenbosch, R.A.J., EthoVision, 2001. A versatile video tracking system for automation of behavioral experiments. Behav. Res. Methods Instrum. Comput. 33, 398–414.
Lu, R., Wang, H., Liang, Z., Ku, L., O'Donnell, W.T., Li, W., Warren, S.T., Feng, Y., 2004. The fragile X protein controls microtubule-associated protein 1B translation and microtubule stability in brain neuron development. Proc. Natl. Acad. Sci. U. S. A 101, 15201–15206.
Lui, H., Zhang, J., Makinson, S.R., Cahill, M.K., Kelley, K.W., Huang, H.Y., Shang, Y., Oldham, M.C., Martens, L.H., Gao, F., et al., 2016. Progranulin deficiency promotes circuit-specific synaptic pruning by microglia via complement activation. Cell 165, 921–935.
Luo, Y., Shan, G., Guo, W., Smrt, R.D., Johnson, E.B., Li, X., Pfeiffer, R.L., Szulwach, K.E., Duan, R., Barkho, B.Z., et al., 2010. Fragile X mental retardation protein regulates proliferation and differentiation of adult neural stem/progenitor cells. PLoS Genet. 6, e1000898.
Martens, L.H., Zhang, J., Barmada, S.J., Zhou, P., Kamiya, S., Sun, B., Min, S.W., Gan, L., Finkbeiner, S., Huang, E.J., Farese Jr., R.V., 2012. Progranulin deficiency promotes neuroinflammation and neuron loss following toxin-induced injury. J. Clin. Investig. 122, 3955–3959.
Maurin, T., Lebrigand, K., Castagnola, S., Paquet, A., Jarjat, M., Popa, A., Grossi, M., Rage, F., Bardoni, B., 2018. HITS-CLIP in various brain areas reveals new targets and new modalities of RNA binding by fragile X mental retardation protein. Nucleic Acids Res. 46, 6344–6355.
Menon, L., Mader, S.A., Mihailescu, M.R., 2008. Fragile X mental retardation protein interactions with the microtubule associated protein 1B RNA. RNA 14, 1644–1655.
Mineur, Y.S., Sluyter, F., de Wit, S., Oostra, B.A., Crusio, W.E., 2002. Behavioral and neuroanatomical characterization of the Fmr1 knockout mouse. Hippocampus 12, 39–46.
Moessner, R., Marshall, C.R., Sutcliffe, J.S., Skaug, J., Pinto, D., Vincent, J., Zwaigenbaum, L., Fernandez, B., Roberts, W., Szatmari, P., Scherer, S.W., 2007. Contribution of SHANK3 mutations to autism spectrum disorder. Am. J. Hum. Genet. 81, 1289–1297.
Nicoletto, B.B., Canani, L.H., 2015. The role of progranulin in diabetes and kidney disease. Diabetol. Metab. Syndrome 7, 117.
Nielsen, D.M., Derber, W.J., McClellan, D.A., Crnic, L.S., 2002. Alterations in the auditory startle response in Fmr1 targeted mutant mouse models of fragile X syndrome. Brain Res. 927, 8–17.
Nimchinsky, E.A., Oberlander, A.M., Svoboda, K., 2001. Abnormal development of dendritic spines in FMR1 knock-out mice. J. Neurosci. 21, 5139–5146.
Park, S.Y., Kim, D., Kee, S.H., 2019. Metformin-activated AMPK regulates β-catenin to reduce cell proliferation in colon carcinoma RKO cells. Oncol. Lett. 17, 2695–2702.
Paushter, D.H., Du, H., Feng, T., Hu, F., 2018. The lysosomal function of progranulin, a guardian against neurodegeneration. Acta Neuropathol. 136, 1–17.
Peça, J., Feliciano, C., Ting, J.T., Wang, W., Wells, M.F., Venkatraman, T.N., Lascola, C. D., Fu, Z., Feng, G., 2011. Shank3 mutant mice display autistic-like behaviours and striatal dysfunction. Nature 472, 437–442.
Pedini, G., Buccarelli, M., Bianchi, F., Pacini, L., Cencelli, G., D'Alessandris, Q.G., Martini, M., Giannetti, S., Sasso, F., Melocchi, V., et al., 2022. FMRP modulates the Wnt signalling pathway in glioblastoma. Cell Death Dis. 13, 719.
Petkau, T.L., Neal, S.J., Milnerwood, A., Mew, A., Hill, A.M., Orban, P., Gregg, J., Lu, G., Feldman, H.H., Mackenzie, I.R., et al., 2012. Synaptic dysfunction in progranulin-deficient mice. Neurobiol. Dis. 45, 711–722.
Petkau, T.L., Life, B., Lu, G., Yang, J., Fornes, O., Wasserman, W., Simpson, E.M., Leavitt, B.R., 2021. Human progranulin-expressing mice as a novel tool for the development of progranulin-modulating therapeutics. Neurobiol. Dis. 153, 105314.
Petroni, V., Subashi, E., Premoli, M., Wöhr, M., Crusio, W.E., Lemaire, V., Pietropaolo, S., 2022. Autistic-like behavioral effects of prenatal stress in juvenile Fmr1 mice: the relevance of sex differences and gene-environment interactions. Sci. Rep. 12, 7269.
Pieretti, M., Zhang, F.P., Fu, Y.H., Warren, S.T., Oostra, B.A., Caskey, C.T., Nelson, D.L., 1991. Absence of expression of the FMR-1 gene in fragile X syndrome. Cell 66, 817–822.
Piscopo, P., Rivabene, R., Adduci, A., Mallozzi, C., Malvezzi-Campeggi, L., Crestini, A., Confaloni, A., 2010. Hypoxia induces up-regulation of progranulin in neuroblastoma cell lines. Neurochem. Int. 57, 893–898.
Piscopo, P., Grasso, M., Fontana, F., Crestini, A., Puopolo, M., Del Vescovo, V., Venerosi, A., Calamandrei, G., Vencken, S.F., Greene, C.M., et al., 2016. Reduced miR-659-3p levels correlate with progranulin increase in hypoxic conditions: implications for frontotemporal dementia. Front. Mol. Neurosci. 9.
Proteau-Lemieux, M., Lacroix, A., Galarneau, L., Corbin, F., Lepage, J.-F., Çaku, A., 2021. The safety and efficacy of metformin in fragile X syndrome: an open-label study. Prog. Neuro Psychopharmacol. Biol. Psychiatr. 110, 110307.
Protic, D., Salcedo-Arellano, M.J., Dy, J.B., Potter, L.A., Hagerman, R.J., 2019a. New targeted treatments for fragile X syndrome. Curr. Pediatr. Rev. 15, 251–258.
Protic, D., Aydin, E.Y., Tassone, F., Tan, M.M., Hagerman, R.J., Schneider, A., 2019b. Cognitive and behavioral improvement in adults with fragile X syndrome treated with metformin-two cases. Mol. Genet. Genom. Med. 7, e00745.
Qu, H., Deng, H., Hu, Z., 2013. Plasma progranulin concentrations are increased in patients with type 2 diabetes and obesity and correlated with insulin resistance. Mediat. Inflamm. 2013, 360190.
Rosen, E.Y., Wexler, E.M., Versano, R., Coppola, G., Gao, F., Winden, K.D., Oldham, M. C., Martens, L.H., Zhou, P., Farese Jr., R.V., Geschwind, D.H., 2011. Functional genomic analyses identify pathways dysregulated by progranulin deficiency, implicating Wnt signaling. Neuron 71, 1030–1042.
Rudelli, R.D., Brown, W.T., Wisniewski, K., Jenkins, E.C., Laure-Kamionowska, M., Connell, F., Wisniewski, H.M., 1985. Adult fragile X syndrome. Clinico-neuropathologic findings. Acta Neuropathol. 67, 289–295.
Saré, R.M., Levine, M., Smith, C.B., 2016. Behavioral phenotype of Fmr1 knock-out mice during active phase in an altered light/dark cycle. eNeuro 3.
Sawicka, K., Pyronneau, A., Chao, M., Bennett, M.V., Zukin, R.S., 2016. Elevated ERK/p90 ribosomal S6 kinase activity underlies audiogenic seizure susceptibility in fragile X mice. Proc. Natl. Acad. Sci. U. S. A 113, E6290–e6297.
She, A., Kurtser, I., Reis, S.A., Hennig, K., Lai, J., Lang, A., Zhao, W.-N., Mazitschek, R., Dickerson, B.C., Herz, J., Haggarty, S.J., 2017. Selectivity and kinetic requirements of HDAC inhibitors as progranulin enhancers for treating frontotemporal dementia. Cell Chem. Biol. 24, 892–906.e895.
Sidhu, H., Dansie, L.E., Hickmott, P.W., Ethell, D.W., Ethell, I.M., 2014. Genetic removal of matrix metalloproteinase 9 rescues the symptoms of fragile X syndrome in a mouse model. J. Neurosci. : the official journal of the Society for Neuroscience 34, 9867–9879.
Siomi, H., Siomi, M.C., Nussbaum, R.L., Dreyfuss, G., 1993. The protein product of the fragile X gene, FMR1, has characteristics of an RNA-binding protein. Cell 74, 291–298.
Slegtenhorst-Eegdeman, K.E., de Rooij, D.G., Verhoef-Post, M., van de Kant, H.J.G., Bakker, C.E., Oostra, B.A., Grootegoed, J.A., Themmen, A.P.N., 1998. Macroorchidism in FMR1 knockout mice is caused by increased Sertoli cell proliferation during testicular development*. Endocrinology 139, 156–162.
Smith, K.R., Damiano, J., Franceschetti, S., Carpenter, S., Canafoglia, L., Morbin, M., Rossi, G., Pareyson, D., Mole, S.E., Staropoli, J.F., et al., 2012. Strikingly different clinicopathological phenotypes determined by progranulin-mutation dosage. Am. J. Hum. Genet. 90, 1102–1107.
Su, T., Fan, H.X., Jiang, T., Sun, W.W., Den Wy, Gao, M.M., Chen, S.Q., Zhao, Q.H., Yi, Y. H., 2011. Early continuous inhibition of group 1 mGlu signaling partially rescues dendritic spine abnormalities in the Fmr1 knockout mouse model for fragile X syndrome. Psychopharmacology (Berl) 215, 291–300.
Tanaka, Y., Suzuki, G., Matsuwaki, T., Hosokawa, M., Serrano, G., Beach, T.G., Yamanouchi, K., Hasegawa, M., Nishihara, M., 2017. Progranulin regulates lysosomal function and biogenesis through acidification of lysosomes. Hum. Mol. Genet. 26, 969–988.
Teo, J.-L., Kahn, M., 2010. The Wnt signaling pathway in cellular proliferation and differentiation: a tale of two coactivators. Adv. Drug Deliv. Rev. 62, 1149–1155.
The Dutch-Belgian Fragile, X.C., Bakker, C.E., Verheij, C., Willemsen, R., van der Helm, R., Oerlemans, F., Vermey, M., Bygrave, A., Hoogeveen, A., Oostra, B.A., et al., 1994. Fmr1 knockout mice: a model to study fragile X mental retardation. Cell 78, 23–33.
Turner, G., Eastman, C., Casey, J., McLeay, A., Procopis, P., Turner, B., 1975. X-linked mental retardation associated with macro-orchidism. J. Med. Genet. 12, 367–371.
Van Damme, P., Van Hoecke, A., Lambrechts, D., Vanacker, P., Bogaert, E., van Swieten, J., Carmeliet, P., Van Den Bosch, L., Robberecht, W., 2008. Progranulin functions as a neurotrophic factor to regulate neurite outgrowth and enhance neuronal survival. J. Cell Biol. 181, 37–41.
Vandesompele, J., De Preter, K., Pattyn, F., Poppe, B., Van Roy, N., De Paepe, A., Speleman, F., 2002. Accurate normalization of real-time quantitative RT-PCR data by geometric averaging of multiple internal control genes. Genome Biol. 3 research0034.0031.
Vasuta, C., Caunt, C., James, R., Samadi, S., Schibuk, E., Kannangara, T., Titterness, A.K., Christie, B.R., 2007. Effects of exercise on NMDA receptor subunit contributions to bidirectional synaptic plasticity in the mouse dentate gyrus. Hippocampus 17, 1201–1208.
Verheij, C., Bakker, C.E., de Graaff, E., Keulemans, J., Willemsen, R., Verkerk, A.J., Galjaard, H., Reuser, A.J., Hoogeveen, A.T., Oostra, B.A., 1993. Characterization and localization of the FMR-1 gene product associated with fragile X syndrome. Nature 363, 722–724.
Verkerk, A.J.M.H., Pieretti, M., Sutcliffe, J.S., Fu, Y.-H., Kuhl, D.P.A., Pizzuti, A., Reiner, O., Richards, S., Victoria, M.F., Zhang, F., et al., 1991. Identification of a gene (FMR-1) containing a CGG repeat coincident with a breakpoint cluster region exhibiting length variation in fragile X syndrome. Cell 65, 905–914.
Waga, C., Okamoto, N., Ondo, Y., Fukumura-Kato, R., Goto, Y., Kohsaka, S., Uchino, S., 2011. Novel variants of the SHANK3 gene in Japanese autistic patients with severe delayed speech development. Psychiatr. Genet. 21, 208–211.
Wang, X., McCoy, P.A., Rodriguiz, R.M., Pan, Y., Je, H.S., Roberts, A.C., Kim, C.J., Berrios, J., Colvin, J.S., Bousquet-Moore, D., et al., 2011. Synaptic dysfunction and abnormal behaviors in mice lacking major isoforms of Shank3. Hum. Mol. Genet. 20, 3093–3108.
Wang, X., Snape, M., Klann, E., Stone, J.G., Singh, A., Petersen, R.B., Castellani, R.J., Casadesus, G., Smith, M.A., Zhu, X., 2012. Activation of the extracellular signal-regulated kinase pathway contributes to the behavioral deficit of fragile x-syndrome. J. Neurochem. 121, 672–679.

Wang, L., Chen, J., Hu, Y., Liao, A., Zheng, W., Wang, X., Lan, J., Shen, J., Wang, S., Yang, F., et al., 2022. Progranulin improves neural development via the PI3K/Akt/GSK-3β pathway in the cerebellum of a VPA-induced rat model of ASD. Transl. Psychiatry 12, 114.

Wen, T.H., Afroz, S., Reinhard, S.M., Palacios, A.R., Tapia, K., Binder, D.K., Razak, K.A., Ethell, I.M., 2018. Genetic reduction of matrix metalloproteinase-9 promotes formation of perineuronal nets around parvalbumin-expressing interneurons and normalizes auditory cortex responses in developing Fmr1 knock-out mice. Cerebr. Cortex 28, 3951–3964.

Xiong, Z.S., Gong, S.F., Si, W., Jiang, T., Li, Q.L., Wang, T.J., Wang, W.J., Wu, R.Y., Jiang, K., 2019. Effect of metformin on cell proliferation, apoptosis, migration and invasion in A172 glioma cells and its mechanisms. Mol. Med. Rep. 20, 887–894.

Xu, S.Q., Tang, D., Chamberlain, S., Pronk, G., Masiarz, F.R., Kaur, S., Prisco, M., Zanocco-Marani, T., Baserga, R., 1998. The granulin/epithelin precursor abrogates the requirement for the insulin-like growth factor 1 receptor for growth in vitro. J. Biol. Chem. 273, 20078–20083.

Yan, Q.J., Asafo-Adjei, P.K., Arnold, H.M., Brown, R.E., Bauchwitz, R.P., 2004. A phenotypic and molecular characterization of the fmr1-tm1Cgr fragile X mouse. Gene Brain Behav. 3, 337–359.

Yang, E.-J., Ahn, S., Lee, K., Mahmood, U., Kim, H.-S., 2016. Early behavioral abnormalities and perinatal alterations of PTEN/AKT pathway in valproic acid autism model mice. PLoS One 11, e0153298.

Yau, S.-Y., Bettio, L., Chiu, J., Chiu, C., Christie, B.R., 2019. Fragile-X syndrome is associated with NMDA receptor hypofunction and reduced dendritic complexity in mature dentate granule cells. Front. Mol. Neurosci. 11.

Yin, F., Banerjee, R., Thomas, B., Zhou, P., Qian, L., Jia, T., Ma, X., Ma, Y., Iadecola, C., Beal, M.F., et al., 2009. Exaggerated inflammation, impaired host defense, and neuropathology in progranulin-deficient mice. J. Exp. Med. 207, 117–128.

Youn, B.S., Bang, S.I., Kloting, N., Park, J.W., Lee, N., Oh, J.E., Pi, K.B., Lee, T.H., Ruschke, K., Fasshauer, M., et al., 2009. Serum progranulin concentrations may be associated with macrophage infiltration into omental adipose tissue. Diabetes 58, 627–636.

Yuskaitis, C.J., Mines, M.A., King, M.K., Sweatt, J.D., Miller, C.A., Jope, R.S., 2010. Lithium ameliorates altered glycogen synthase kinase-3 and behavior in a mouse model of fragile X syndrome. Biochem. Pharmacol. 79, 632–646.

Zanocco-Marani, T., Bateman, A., Romano, G., Valentinis, B., He, Z.-H., Baserga, R., 1999. Biological activities and signaling pathways of the granulin/epithelin Precursor1. Cancer Res. 59, 5331–5340.

Zhang, M., Wang, Q., Huang, Y., 2007. Fragile X mental retardation protein FMRP and the RNA export factor NXF2 associate with and destabilize Nxf1 mRNA in neuronal cells. Proc. Natl. Acad. Sci. U. S. A 104, 10057–10062.

Zhang, K., Li, Y.J., Guo, Y., Zheng, K.Y., Yang, Q., Yang, L., Wang, X.S., Song, Q., Chen, T., Zhuo, M., Zhao, M.G., 2017. Elevated progranulin contributes to synaptic and learning deficit due to loss of fragile X mental retardation protein. Brain 140, 3215–3232.

Zhao, M.-G., Toyoda, H., Ko, S.W., Ding, H.-K., Wu, L.-J., Zhuo, M., 2005. Deficits in trace fear memory and long-term potentiation in a mouse model for fragile X syndrome. J. Neurosci. 25, 7385.